

Freeze Stage Analysis of an Indirect Freeze Desalination System

by
Trevor A. Whitaker

A THESIS

submitted to

Oregon State University

University Honors College

in partial fulfillment of
the requirements for the
degree of

Honors Bachelors of Science in Mechanical Engineering
Honors Associate

Presented March 11, 2019
Commencement June 2019

AN ABSTRACT OF THE THESIS OF

Trevor A. Whitaker for the degree of Honors Baccalaureate of Science in Mechanical Engineering presented on March 11, 2019

Title: Freezing Process Analysis for Indirect Freeze Desalination System

Abstract Approved: _____

Deborah V. Pence
Thermal-Fluid Sciences

Freeze desalination poses as a potential solution to many of the issues that accompany current desalination methods. The research detailed in this manuscript involves creating and analyzing a numerical model of the freezing operation of an indirect contact freeze-melting (FM) desalination system. In this initial analysis, pure water is frozen to avoid the need to model mass transfer within the saltwater. The system consists of a single vertical tube submerged in a chamber of water. Coolant enters the tube at a set inlet temperature below the freezing point of water, causing ice to form on the outer surface of the tube. In order to analyze how the system reacts to changes; cycle time, mass flow rate, overall tube length, and tube radius were varied parametrically. Because the thermal resistance of the ice layer increases with time—slowing the ice production rate—the optimal cycle time was determined to be 1,500 seconds when changeover between freezing and melting cycles was accounted for.

Key Words: freeze desalination, direct contact, numerical model, modular, mobile
Corresponding E-mail Address: whitaket@oregonstate.edu

©Copyright by Trevor A. Whitaker
March 11, 2019
All Rights Reserved

Freeze Stage Analysis of an Indirect Freeze Desalination System

by
Trevor A. Whitaker

A THESIS

submitted to

Oregon State University

University Honors College

in partial fulfillment of
the requirements for the
degree of

Honors Bachelors of Science in Mechanical Engineering
Honors Associate

Presented March 11, 2019
Commencement June 2019

Honors Baccalaureate of Science in Mechanical Engineering thesis of
Trevor A. Whitaker presented on March 11, 2019

APPROVED:

Deborah V. Pence
Mentor, representing Thermal-Fluid Sciences

James Liburdy
Committee Member, representing Thermal-Fluid Sciences

Joshua Gess
Committee Member, representing Thermal-Fluid Sciences

Toni Doolen
Dean, Oregon State University Honors College

I understand that my thesis will become part of the permanent collection of Oregon State University libraries. My signature below authorizes release of my thesis to any reader upon request.

Trevor A. Whitaker, Author

ACKNOWLEDGEMENTS

First and foremost, I would like to thank my advisor, Dr. Deborah Pence. Without your guidance and help throughout this process, it is doubtful I would have seen a meaningful conclusion to this project. You have kept me motivated and excited about this project and pushed me to its completion.

I am grateful for my senior capstone group members, and moreover, some of my closest friends Mason Pratt, Josh Cook, and Francisco Boschetti. Your help on this project was pivotal to its success, and I truly could not have done it without all of you.

Finally, to my wife Ryanne. You have been my emotional support through the entirety of my undergraduate degree. I cannot thank you enough for always being there.

Thank you to everyone for your help.

TABLE OF CONTENTS

LIST OF FIGURES	2
LIST OF TABLES	3
NOMENCLATURE	4
1 INTRODUCTION	6
1.1 Necessity for Desalination	6
1.2 Proposed System	7
1.3 Scope of Analysis	10
1.4 Project Goals	10
2 BACKGROUND	11
2.1 Overview of Alternative Desalination Methods	11
2.1.1 Reverse Osmosis	11
2.1.2 Multistage Flash	12
2.1.3 Mechanical Vapor Compression	13
2.2 Overview of Freeze Desalination	14
2.2.1 History	14
2.2.2 FM Processes	16
2.3 Related Work	17
3 METHODOLOGY	19
3.1 Steady-State Global Analysis	20
3.2 Transient Global Analysis	21
3.3 Spacial-Temporal Analysis	31
4 RESULTS & DISCUSSION	33
5 CONCLUSIONS & RECOMMENDATIONS	47
REFERENCES	51
APPENDICES	52
Appendix A - Spacial-Temporal Analysis Code	52
Appendix B - Transient Global Analysis Code	57
Appendix C - Steady-State Analysis Code	61
Appendix D - Convergence Analysis Code	63
Appendix E - Base Case System Constants	66

LIST OF FIGURES

1	Freeze chamber conceptual diagram.	9
2	Vertical cross section of the general control volume, from tube centerline radially outward to feed water.	20
3	Control volume 1, around the ice phase change region.	23
4	Control volume 2, at the interface between the outer tube wall and ice.	24
5	Control volume 3, at the interface between the inner tube wall and coolant.	26
6	Control volume 4, around the coolant in the tube.	28
7	Tested conditions for δL and δt convergence.	35
8	Volume of ice produced as a function of time at vertices of figure 7. Note that the code iterates in time between 0 and $(1500 - \delta t)$ seconds. This is not an issue at small time steps, but at larger time steps, the cycle time is cut short.	35
9	Ice production as a function of time for all three analyses.	36
10	Ice growth profile along the tube length as a function of time.	38
11	Conductive resistance of ice layer as a function of time at different points along the tube length.	38
12	Coolant heat removal rate with respect to time at base case.	39
13	Ice profile along the length of the tube with varying coolant mass flow rate. Note that because the x-axis does not begin at zero, the shape of the ice profile is exaggerated.	41
14	Volume of ice produced as a function of coolant mass flow rate.	42
16	Chiller power requirement as a function of tube length.	43
15	Volume of ice produced as a function of time with varying tube length.	43
17	Volume of ice produced as a function of tube radius with tube thickness held constant.	45

LIST OF TABLES

1	Requirements of the different desalination methods. ✓ indicates presence of indicated complication, ✗ indicates the absence thereof.	15
2	Base case (B.C.) values.	33
3	Base case (B.C.) constants.	66

NOMENCLATURE

Symbols

Δt	Time step [s]
\dot{m}	Mass flow rate [kg/s]
λ	Enthalpy [J/kg]
ρ	Density [kg/m ³]
c	Specific heat [J/kg-C]
E	Energy [J]
h	Convective heat transfer coefficient [W/m ² -C]
k	Conductive heat transfer coefficient [W/m-C]
L	Length [m]
R	Thermal Resistance [C/W]
r	Radius [m]
T	Temperature [C]
t	Time [s]
U	Internal Energy [J]
V	Volume [m ³]

Subscripts

inf	Property of water in freeze chamber
adv	Advection
Avg	Calculated average property between length steps of pipe
A	Property at surface of inner pipe wall
B	Property at surface of outer pipe wall
$cond$	Conduction
$conv$	Convection
C	Property at outer surface of ice

<i>ice</i>	Property of ice formed
<i>in</i>	Property at freeze chamber pipe inlet
<i>i</i>	Property at length increment <i>i</i>
<i>out</i>	Property at freeze chamber pipe outlet
<i>pc</i>	Property of water phase change region
<i>R</i>	Property of system cooling fluid
<i>sf</i>	Property of phase change for water from fluid to solid
<i>s</i>	Property of water
<i>w</i>	Property of pipe material

Superscripts

<i>k</i>	Property at time step <i>k</i>
----------	--------------------------------

1 INTRODUCTION

1.1 Necessity for Desalination

Due to the rapidly growing population, humanity's access to freshwater is becoming increasingly limited. Freshwater makes up only 2.5% of the total water on the planet, and almost 70% of all freshwater is found frozen in glaciers and ice caps [1]. One of the major issues society will face in the near future is groundwater depletion caused by removing water from the water table (the region underground where pores in the soil are filled with water) at a faster rate than can be replenished naturally. When this occurs, the level of the water table is lowered and—if the area is in close enough proximity to a source of saltwater—the freshwater will essentially be replaced by saltwater [2]. In an agricultural setting, this can be especially detrimental because crops cannot be irrigated with brackish water; the most resilient crops have a salinity tolerance of less than 460ppm [3]. Produce growers like those in California are in desperate need of a solution to this issue before they can no longer grow crops.

The personal human need for freshwater raises a similar concern as the increasing population creates an even greater need for, and depletion of, fresh water supplies. While no exact acceptable concentration for drinking water has been established, in general, water is only considered fresh at salinity levels lower than $1,000\text{ppm}$ [4] and municipal tap water is usually found containing a salinity of

less than 100ppm . With typical seawater containing approximately $35,000\text{ppm}$, a reduction of at least 97% is necessary to obtain useable freshwater [5].

Although technology for saltwater desalination already exists, processes currently used are energy intensive, prone to failures, and potentially harmful to the environment. Some of the most prominent methods employed are reverse osmosis (RO), multistage flash desalination (MSF), and mechanical vapor compression (MVC). Freeze desalination is particularly interesting because it provides a possible solution to many of the issues related to the aforementioned processes. The overall aim of this work conducted at Oregon State University is to develop a small-scale, deployable, solar-assisted freeze desalination unit that can easily be transported to farms or used in disaster scenarios (such as hurricanes or flooding) as an effective, short term solution to a lack of necessary freshwater. This project is a preliminary analysis aiming to determine whether indirect freeze desalination is a feasible solution in these cases, where cost effectiveness, production capacity, reliability, and environmental impact are the metrics for determining its practicality.

1.2 Proposed System

The system considered in this thesis is a single stage of a multistage tube-in-tank indirect freeze desalination unit. While other methods of freeze desalination may be more effective in an industrial setting, the indirect method was chosen for its viability at small scale as well as the straightforwardness of the process [6].

A visualization of the system can be seen in figure 1. In this system, a chilled mixture of water and ethylene glycol is pumped through the tubes, cooling the saltwater in the tank. As energy is removed, ice begins to precipitate on the outer surfaces of the tubes. While the ice that is formed is relatively pure, a salty slurry layer will remain on the outer surface of the ice even after the residual liquid water has been drained from the tank. In the typical method, the ice would be washed or put in a centrifuge to remove any brine left on the outer surfaces; however, a staging method is proposed in this project to further desalinate the water to concentrations suitable for human or agricultural use. Similar indirect freezing experiments give expected values for final salinity of the product water after a single stage [7]. Based on the number of cycles required to lower the salinity to acceptable levels, total required energy per unit volume of clean water produced can be roughly determined. An outdoor ethylene glycol chiller is used to supply the cooling fluid to the freeze chamber. After the freezing cycle is run, a heating unit will warm and pump the ethylene glycol mixture through the same tubes, melting the ice and allowing the clean water to be harvested. Only the freezing process is studied in the present work, but Mason Pratt [8] analyzes the system melting process in a thesis written in parallel with this one.

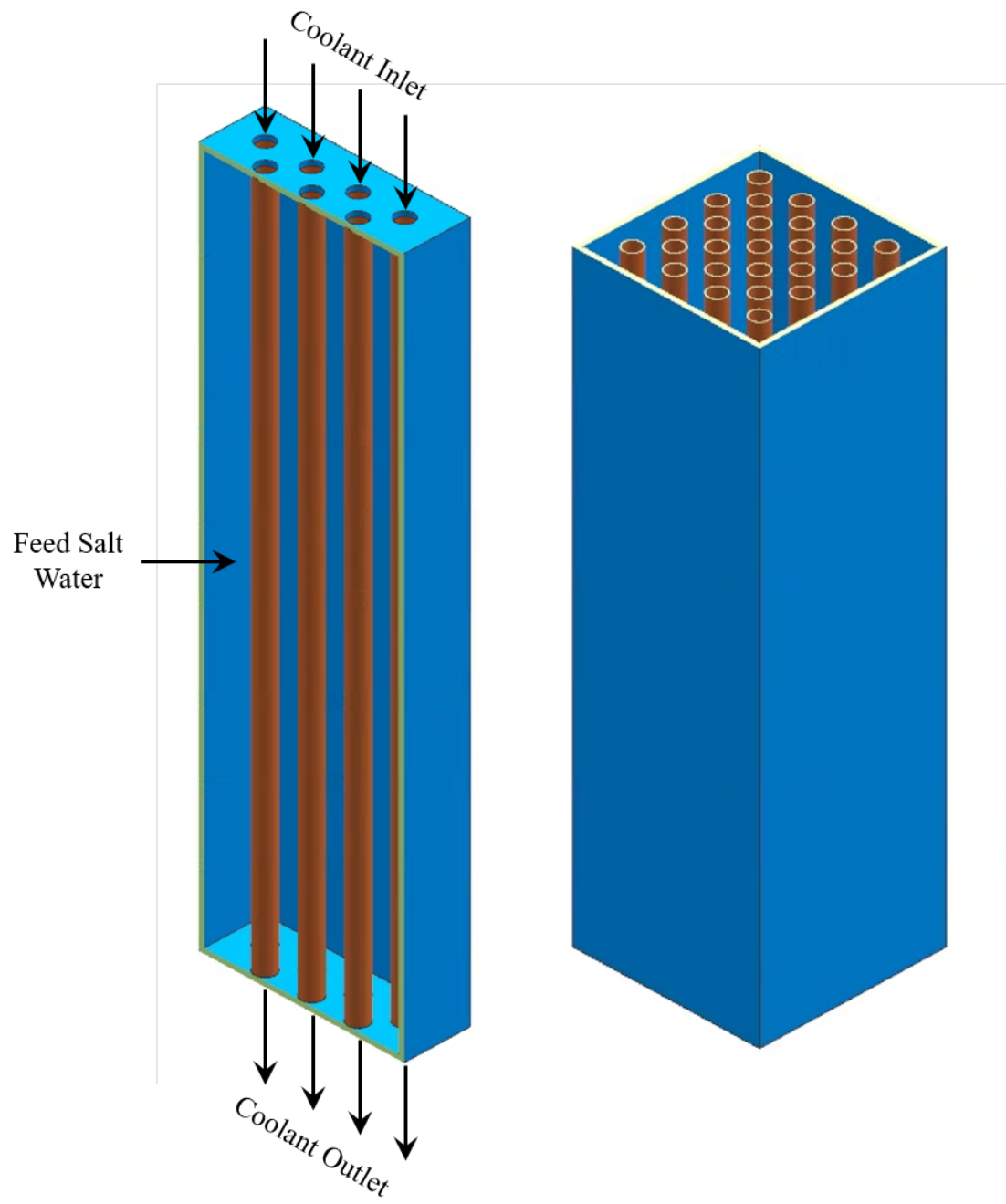


Figure 1: Freeze chamber conceptual diagram.

1.3 Scope of Analysis

The analysis presented in this paper will focus only on the freezing portion of this process. It will determine the energy requirements to operate the freeze chamber optimized for geometric design, ice thickness, and cycle time. A computer-based numerical model of a single tube in the freeze chamber during the freezing cycle of the proposed system will be developed. Neither the overall system design (anything outside of the freeze chamber), nor the solar assistance, nor the component specifications will be presented in this manuscript. While these aspects of the system are not determined within the scope of this particular research, other projects are being conducted in parallel that will provide the necessary specifications to complete the freezing analysis. For more details on this related work, refer to chapter 2.3, presented later in the manuscript.

1.4 Project Goals

The purpose of this research is to develop a computer based model of a tube-in-tank indirect freeze desalination unit and analyze its overall efficacy. Analyzing this system will provide a precursory indication of viability and help to determine if further work on the project is warranted. Should the analysis show promise, it could be used to guide the design of an experimental model that could in turn validate the analysis conducted for this thesis.

2 BACKGROUND

2.1 Overview of Alternative Desalination Methods

A multitude of methods are currently used to desalinate water. With each method having its own unique benefits, there is no clear determination of a single “best” method for desalination. The most prominently used methods today are reverse osmosis (RO), multistage flash (MSF), and mechanical vapor compression (MVC) [9]. For the purposes of this research, the energy consumption, reliability, and relative cost of these methods will serve as benchmarks for the designed system.

2.1.1 Reverse Osmosis

The reverse osmosis method is one of the most promising methods for desalination at the moment. As membrane technology improves and material costs decrease the process only becomes more efficient and cost effective. This process utilizes several semipermeable membranes and a high driving pressure to filter contaminants out of the feed saltwater. The feed water must first undergo a pretreatment process to reduce membrane fouling. Pretreated water is then forced through several membranes, each being less permeable than the previous one until the desired desalination effect is achieved. The energy requirement for this process is between 2.5 and $7\frac{kWh}{m^3}$, depending on feed water salinity [9].

While the method often serves as a benchmark for other desalination processes, and is constantly being improved upon, there are several major issues that still hinder the effectiveness of RO. Membrane fouling causes reduced system reliability and higher energy consumption over time, which necessitates the high level of pretreatment the feed water must undergo prior to filtering. As the initial feed water quality decreases (contains more contaminants) a higher amount of pretreatment is required and potential for fouling increases. Additionally, as salinity of the feed water increases, so too do the power requirements of the operation. For this reason, RO processes do not perform as well at the high salinity levels found in oceanic waters [9].

2.1.2 Multistage Flash

Multistage flash desalination uses a vacuum and added heat to vaporize feed water multiple times, removing a portion of the dissolved salts at each stage. The feed water is first vaporized then cooled and condensed where it can be collected and sent to the next stage. Since both salts and contaminants are removed during the vaporization process (contaminants remain in the liquid water), little to no pretreatment is required for this operation. Another major benefit of this process is that it utilizes low-quality energy (heat) and can have lower energy costs than electrically powered processes, especially in warmer climates. The energy requirement for this process is between 3 and $5 \frac{kWh}{m^3}$ [9].

Disadvantages of MSF and other thermal desalination processes are the high theoretical energy costs as well as issues with scale deposition on components. The theoretical minimum energy required to vaporize a kilogram of water is nearly seven times greater than what is required to freeze the same mass of water [10]. High operating temperatures create more opportunity for scaling which can decrease component longevity as well as reduce overall system efficiency [9]. Additionally, the benefit of using low-quality energy is only realized if there exists a nearby source for this energy (be it waste energy from another thermal process, solar, etc.), which can be difficult to procure in remote areas where a deployable system may be needed.

2.1.3 Mechanical Vapor Compression

The final major non-freezing desalination method that will be highlighted in this thesis is mechanical vapor compression (MVC). This is another distillation process that heats and vaporizes the feed salt water by compressing a working vapor to give off heat. MVC has the unique advantage of being able to use the product steam created during the process as the working vapor for compression. This process, like MSF, requires little to no pretreatment, but its main source of energy consumption is electrical as opposed to thermal. MVC is also capable of operating at high feed water salinity. The energy requirement for this process is between 8 and $15 \frac{kWh}{m^3}$ which is the highest of the more common methods. This process shares the same issues that MSF experiences along with some of its

own: these systems only work well on a small scale, and have high-quality/high-magnitude energy requirements [9].

2.2 Overview of Freeze Desalination

2.2.1 History

Records of sailors using freezing for the express purpose of water desalination can be found dating back to the 17th century [11], although most scientific progress made in the area of freeze desalination did not occur until the mid 20th century [12]. While the process of freeze desalination is relatively straightforward and the potential benefits are well-known, perceived difficulty of ice-brine separation and other misconceptions have caused the method to be overlooked by many as a viable solution to the issue of seawater desalination [13, 14]. Effective methods for washing have been developed that generally require than 5% or less of the total net product water [12]. It cannot necessarily be stated that freezing processes are superior for desalination in all cases, but it can certainly be argued that the promise these methods show warrants more research than has been conducted in the last half century. The major benefits provided by freezing desalination processes are as follows:

- Little to no pretreatment required
- Low operating temperatures reduce sensitivity to scaling and corrosion
- Low sensitivity to changes in salinity or other contaminants in feed water
- Lowest theoretical energy cost of all desalination processes when factors like pretreatment are considered [12]

While the effectiveness of RO processes are negatively impacted by increasing salinity and contaminant concentration, freeze desalination processes experience little to no effect when feed water conditions change. Because the freezing operation is also effective at removing other contaminants from the water, there is effectively no pretreatment necessary [10]. Flash and vapor compression methods offer this same advantage, but their high operating temperatures ($< 120^\circ\text{C}$ for MSF and $< 70^\circ\text{C}$ for MVC) makes system components prone to scaling and corrosion [9]. To account for these high operating temperatures, these systems are usually designed with more expensive materials than freeze-melting (FM) processes [10]. The low theoretical energy cost of freezing compared to vaporization (and when pretreatment is considered, compared to RO processes) is possibly the most important benefit that FM processes provide. Combined advantages and disadvantages for all methods are summarized in Table 1.

Table 1: Requirements of the different desalination methods. \checkmark indicates presence of indicated complication, \times indicates the absence thereof.

	RO	MSF	MVC	FM
Energy Cost	Moderate	Moderate	High	Low
Operating Temperature	Low	High	Moderate	Low
Pretreatment Required	\checkmark	\times	\times	\times
Fouling	\checkmark	\times	\times	\times
Corrosion	\times	\checkmark	\checkmark	\times
Washing Required	\times	\times	\times	\checkmark

2.2.2 FM Processes

An indirect FM process indicates one in which the cooling fluid and the feed water never come in to contact with one another. The system generally consists of a refrigeration cycle, a freeze chamber, a melting chamber, and a separator/washer unit. In a simple configuration, cooling fluid is passed through a tube submerged in liquid salt water and ice begins to form on the outer tube surface, known as the heat transfer surface. After the desired volume of ice is produced, it is then washed and melted. This is the simplest FM process, but other methods will have lower energy requirements due to the absence of heat transfer surface thermal resistance that is associated with the indirect method. Along with increased energy cost, the necessity for heat transfer surfaces will generally increase the unit capital cost as well [10].

The direct contact process uses a refrigerant that is not soluble in water and puts it in direct contact with the feed water. In one direct contact method cooled, pressurized liquid refrigerant is pumped into the freeze chamber where the higher temperature and lower pressure cause it to vaporize. The heat absorbed by vaporization of the refrigerant causes ice crystals to precipitate and float to the top of the tank. The ice/brine slurry is harvested from the top of the freeze chamber and pumped to the wash unit. The vaporized gas from the freeze chamber is re-compressed and used to melt the product ice. This process is without the disadvantage of heat transfer surfaces as well as the ability to make it a continu-

ous cycle as opposed to the batch cycles of indirect FM. The main disadvantage of a direct contact process is the necessity to separate the refrigerant from the water, as refrigerant contaminated with water will negatively impact compressor performance and water contaminated with refrigerant is non-potable [10, 15].

A different direct contact method, vacuum freezing, is essentially opposite of the MVC method where instead of compressing the refrigerant to vaporize the feed water, the refrigerant is vaporized to freeze the feed water. The vacuum FM process can utilize water as the refrigerant to be vaporized, which allows the process to forgo heat transfer surfaces as the vaporization and freezing can occur in direct contact with one another. In this system, the ice can be harvested, washed, and melted similarly to the direct contact method, without the need to separate the refrigerant and water. The vaporized water is free of contaminants and can be harvested as well by using a compressor and an additional refrigeration cycle to condense the vapor. The major drawbacks of this system are its complexity and capital cost. Specifying compressors for large scale applications of this process is difficult [15].

2.3 Related Work

This thesis will primarily focus on the freezing component of an indirect FM process. However, in order to obtain meaningful information about the process as a whole, additional work must be done in determining component specifications, overall system design, melting process analysis, and system optimization.

The current work was conducted in parallel with two other projects at Oregon State University. A counterpart thesis analyzes the melting portion of the system [8]. Because the work will finish at the same time, for the purposes of the calculations herein, the time and power requirements of the melting process will be assumed to be similar to that of the freezing process where necessary. While the melting process does not directly impact the freezing process, it will be valuable to account for it when considering overall power requirements and daily fresh water production capabilities. For more information specific to the melting process, reference the counterpart thesis [8]. The second project that is related to this manuscript is an overall system design and component specification as part of a capstone design project. The overall design project will yield several size/capacity configurations of the full system (freeze chamber, chiller, heater, generator, and piping network) designed to fit within the space restraints of different transportation modes (semi-truck flatbed trailer, flatbed pickup truck, and standard pickup truck) as well as a consideration for the solar assistance component. Chillers, heaters, and generators were specified to provide the maximum cooling/heating capacity within the space restraints, then a genetic learning algorithm was run on the analysis detailed in this manuscript in order to optimize the modular freeze chambers to match the cooling specifications. For the purpose of this thesis, the base case (B.C.) specifications are those optimized by the genetic learning algorithm for a semi-truck flatbed trailer ($8.5ft. \times 48ft.$ area) with a specified chiller capacity for that configuration ($14000 \frac{BTU}{hr} \approx 4.1kW$).

3 METHODOLOGY

The analyses conducted as a part of this research are based on different control volume analyses of a single tube in the freeze chamber for three scenarios: a steady-state global analysis of the entire tube, a transient analysis of the entire tube, and a transient analysis of differential segments along the length of the tube. As each analysis is more refined than the previous, a practical final result could be obtained while always being able to verify new results with those found in the more simplistic scenarios. As this was a preliminary analysis of this system, several assumptions were used to simplify equations while maintaining reasonable results. A summary of these assumptions is given below:

- The single tube analysis assumes that no tube in the freeze chamber will affect adjacent tubes.
- Differences between properties of salt water and fresh water are neglected.
- Mass transfer of salt during phase change is neglected.
- Constant feed water phase change temperature is assumed.
- Changes in kinetic and potential energies are assumed to be negligible.
- Convection between feed water and ice neglected ($h_{feedwater} = 0$).
- Radial symmetry of the tube and ice growth is assumed.
- Assume liquid water and pipe wall temperature close to phase change temperature at initial conditions.

The general control volume to be analyzed can be seen in figure 2. Since radial symmetry can be assumed, the control volume to be analyzed is a cross section of the tube divided in half at the tube centerline with length L (or in the

case of the length discretized analysis, δL). In this configuration, heat is drawn from the phase change region to form ice through the existing ice layer, then the tube wall, and finally to the coolant that is recirculated through a chiller.

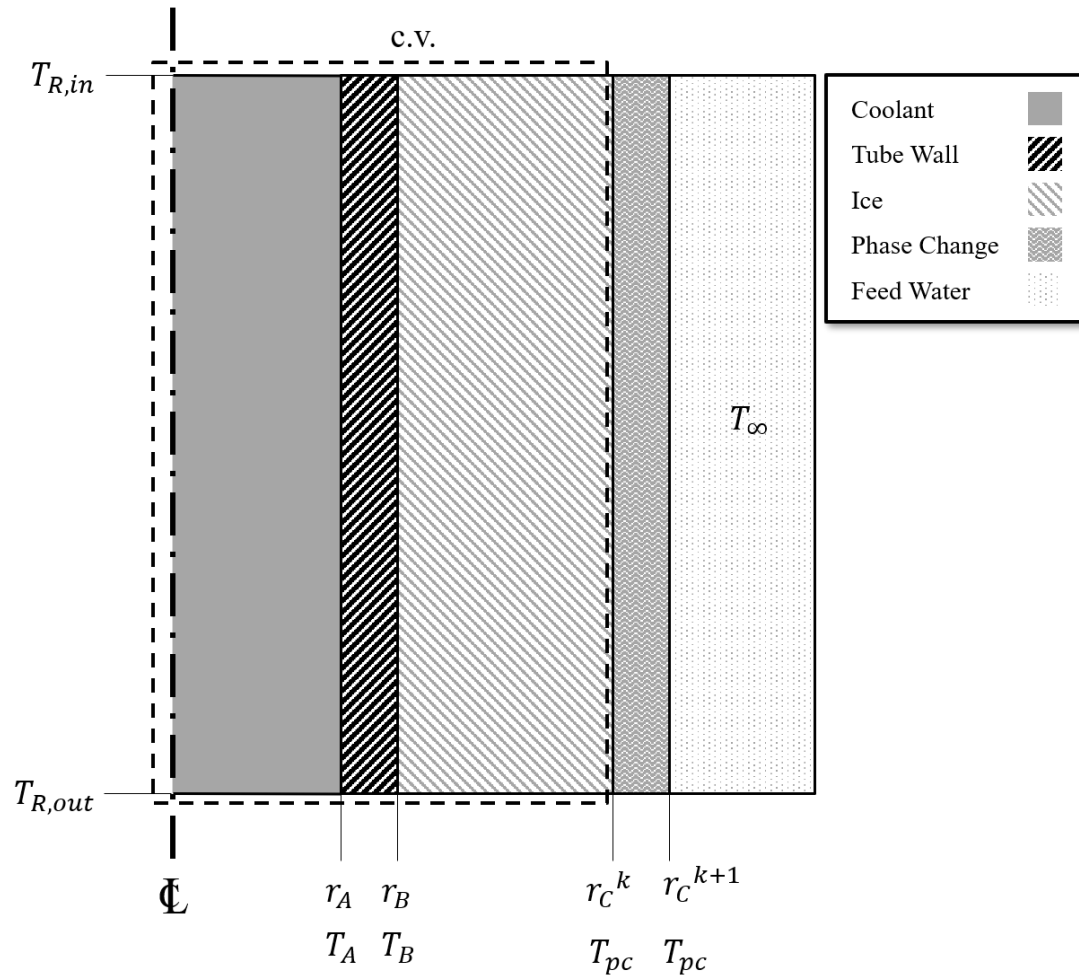


Figure 2: Vertical cross section of the general control volume, from tube centerline radially outward to feed water.

3.1 Steady-State Global Analysis

The steady-state global analysis is both the most simple and least accurate of the three analyses and thus is conducted first to provide a baseline to check

subsequent analyses. Since it is discretized in neither length nor time, it will show ice forming at a constant rate throughout the cycle and constant thickness along the length of the tube. It assumes operation at the maximum heat removal rate (set at 80% of the maximum chiller capacity $3.6kW$) throughout the length of the freezing process. The steady-state global analysis is governed by an energy balance on the entire system shown in figure 2:

$$\frac{dE}{dt} = \dot{Q}_{pc} + \dot{m}_R(h_{R,in} - h_{R,out}) \quad (1)$$

where $\frac{dE}{dt}$ goes to zero. Furthermore, it is assumed that all \dot{Q} , a constant value into the control volume results in ice generation

$$\dot{Q}_{pc} = \frac{\Delta V_{ice} \rho_{ice} \lambda_{sf}}{\Delta t} \quad (2)$$

Written explicitly in terms of the change in volume of ice generated for a specified time increment Δt

$$\Delta V_{ice} = \rho_{ice} \lambda_{sf} \dot{m}_R c_R (T_{R,in} - T_{R,out}) \Delta t \quad (3)$$

where ρ_{ice} , λ_{sf} , \dot{m}_R , c_R , $T_{R,in}$, $T_{R,out}$, and Δt are all knowns.

3.2 Transient Global Analysis

In the transient global analysis, different control volumes are considered that take into consideration the changing thermal resistance of the ice layer as a function

of the ice radius which varies with of time. Therefore, the thermal resistance changes the rate of heat transfer, which influences the coolant exit temperature and must be accounted for in this analysis. The transient global analysis as well as the spacial-temporal analysis assume a linear temperature gradient of the coolant in the tube at the initial condition ($t = 0$). While this is not expected to be reflected in an experimental setup, the duration of the freezing cycle causes the assumption to have a negligible effect on the overall analysis.

Here, several control volumes are considered. First, a control volume around the phase change region of the ice (figure 3), followed by a control volume at the interface between the ice and the outer tube wall (figure 4), at the interface of the inner tube wall and the coolant (figure 5), and finally around the coolant in the tube (figure 6). The energy balance for the phase change region of the ice—neglecting convection between the ice and salt water—can be written as follows:

$$\frac{dE_{phasechange}}{dt} = \dot{Q}_{cond,ice} \quad (4)$$

where

$$\frac{dE_{phasechange}}{dt} \cong \frac{\rho_{ice}\Delta V_{ice}\lambda_{sf}}{\Delta t} \quad (5)$$

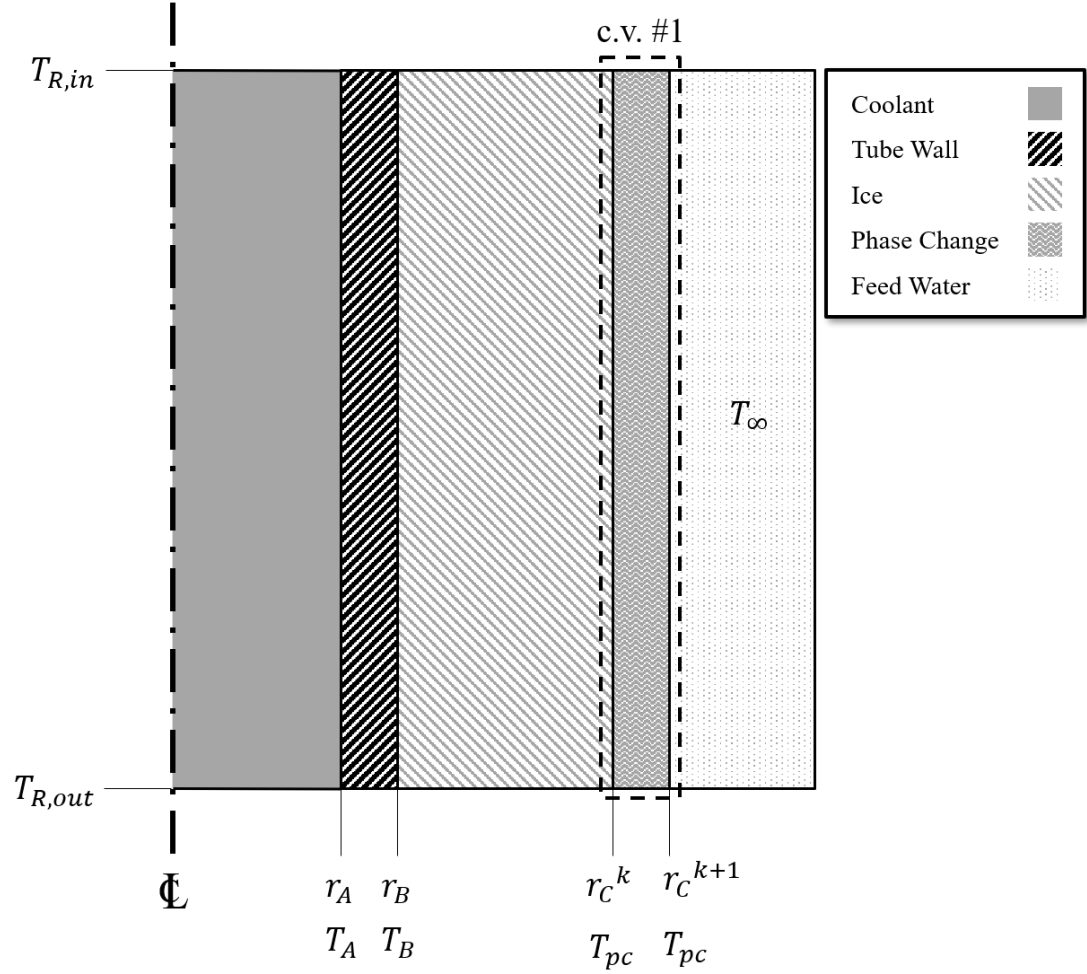


Figure 3: Control volume 1, around the ice phase change region.

and

$$\dot{Q}_{cond,ice} = \frac{\Delta T}{R_{ice}} = \frac{2\pi k_{ice} L}{\ln\left(\frac{r_C^k}{r_B}\right)} (T_{pc} - T_B) \quad (6)$$

such that the energy balance on around the phase change region yields:

$$\frac{\rho_{ice} \Delta V_{ice} \lambda_{sf}}{\Delta t} = \frac{2\pi k_{ice} L}{\ln\left(\frac{r_C^k}{r_B}\right)} (T_{pc} - T_B) \quad (7)$$

Equation 7 has two unknowns: ΔV_{ice} and T_B . In order to solve the equation for ΔV_{ice} , there must exist an equation to solve for T_B . To achieve this, an energy balance is conducted on the outer tube wall. As there is no volume, there is no transient term, such that the tube wall energy balance is:

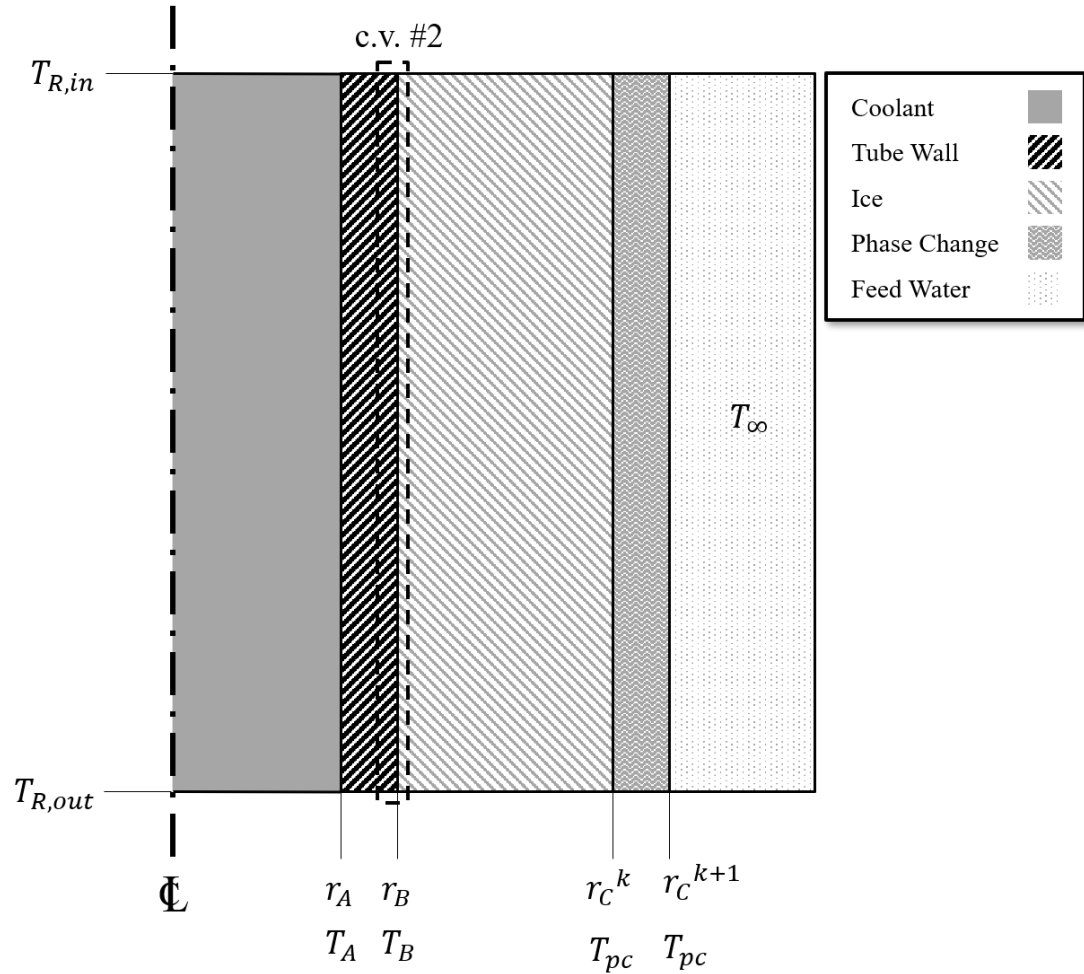


Figure 4: Control volume 2, at the interface between the outer tube wall and ice.

$$\dot{Q}_{cond,ice} = \dot{Q}_{cond,w} \quad (8)$$

$\dot{Q}_{cond,ice}$ is written in equation 6 and $\dot{Q}_{cond,w}$ is

$$\dot{Q}_{cond,w} = \frac{\Delta T}{R_w} = \frac{2\pi k_w L}{\ln\left(\frac{r_B}{r_A}\right)}(T_B - T_A) \quad (9)$$

thus the complete energy balance at the interface between the ice and outer tube wall can be written as

$$\frac{2\pi k_{ice} L}{\ln\left(\frac{r_C}{r_B}\right)}(T_{pc} - T_B) = \frac{2\pi k_w L}{\ln\left(\frac{r_B}{r_A}\right)}(T_B - T_A) \quad (10)$$

This equation presents another unknown: T_A . Another equation must be written in order to solve for T_A . Again, the heat will transfer towards the center of the tube, and an energy balance can be written at the inner wall of the tube:

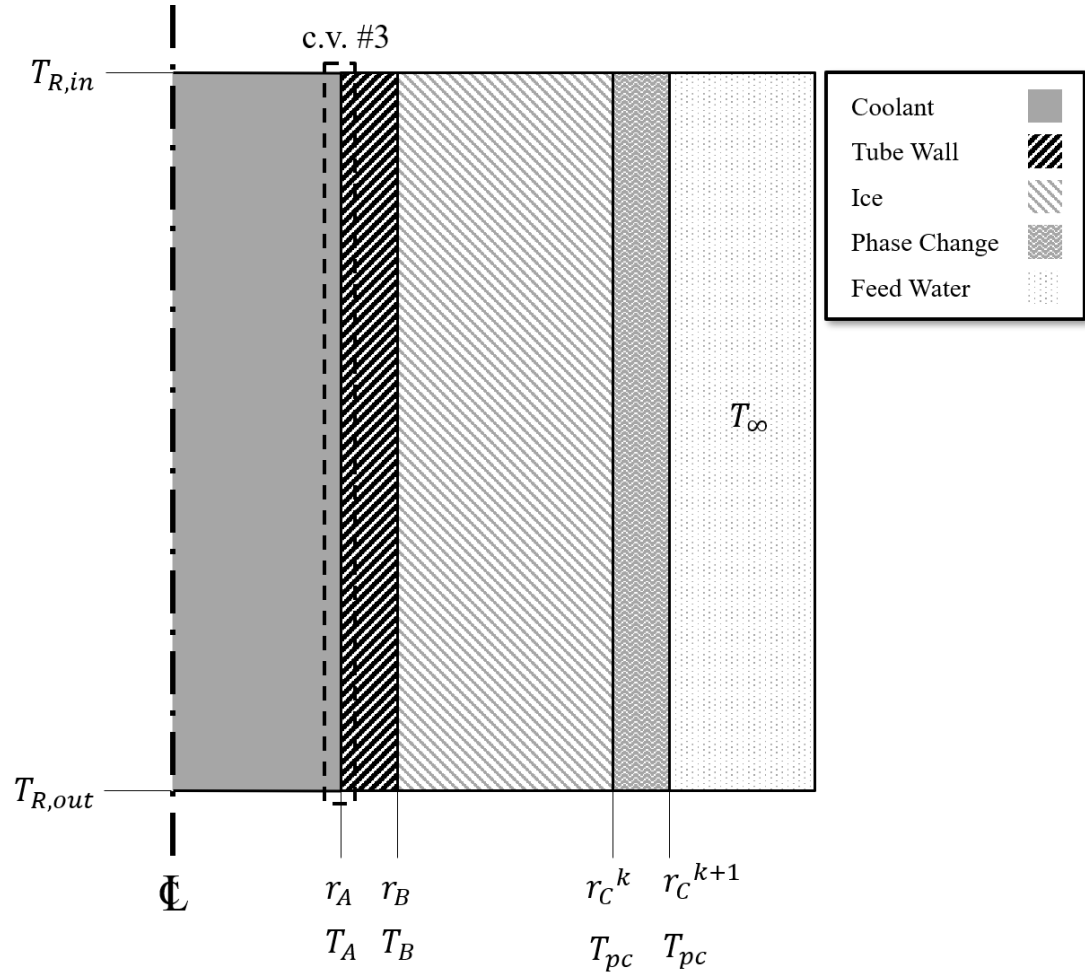


Figure 5: Control volume 3, at the interface between the inner tube wall and coolant.

$$\dot{Q}_{cond,w} = \dot{Q}_{conv,R} \quad (11)$$

The left-hand side of the equation is defined in equation 9, and the right-hand side is written as follows:

$$\dot{Q}_{conv,R} = h_R A \Delta T = 2\pi r_A L h_R (T_A - T_{R,Avg}) \quad (12)$$

such that the energy balance becomes

$$\frac{2\pi k_w L}{\ln\left(\frac{r_B}{r_A}\right)}(T_B - T_A) = 2\pi r_A L h_R (T_A - T_{R,Avg}) \quad (13)$$

In equation 13, $T_{R,Avg}$ represents the average temperature of the cooling fluid that can be written in terms of the known temperature $T_{R,in}$ and the unknown temperature $T_{R,out}$:

$$T_{R,Avg} = \frac{T_{R,in} + T_{R,out}}{2} \quad (14)$$

The last variable to be accounted for is $T_{R,out}$, which can be determined by conducting a final energy balance on the coolant. Neglecting kinetic and potential energy effects, this energy balance on control volume 4 is written as:

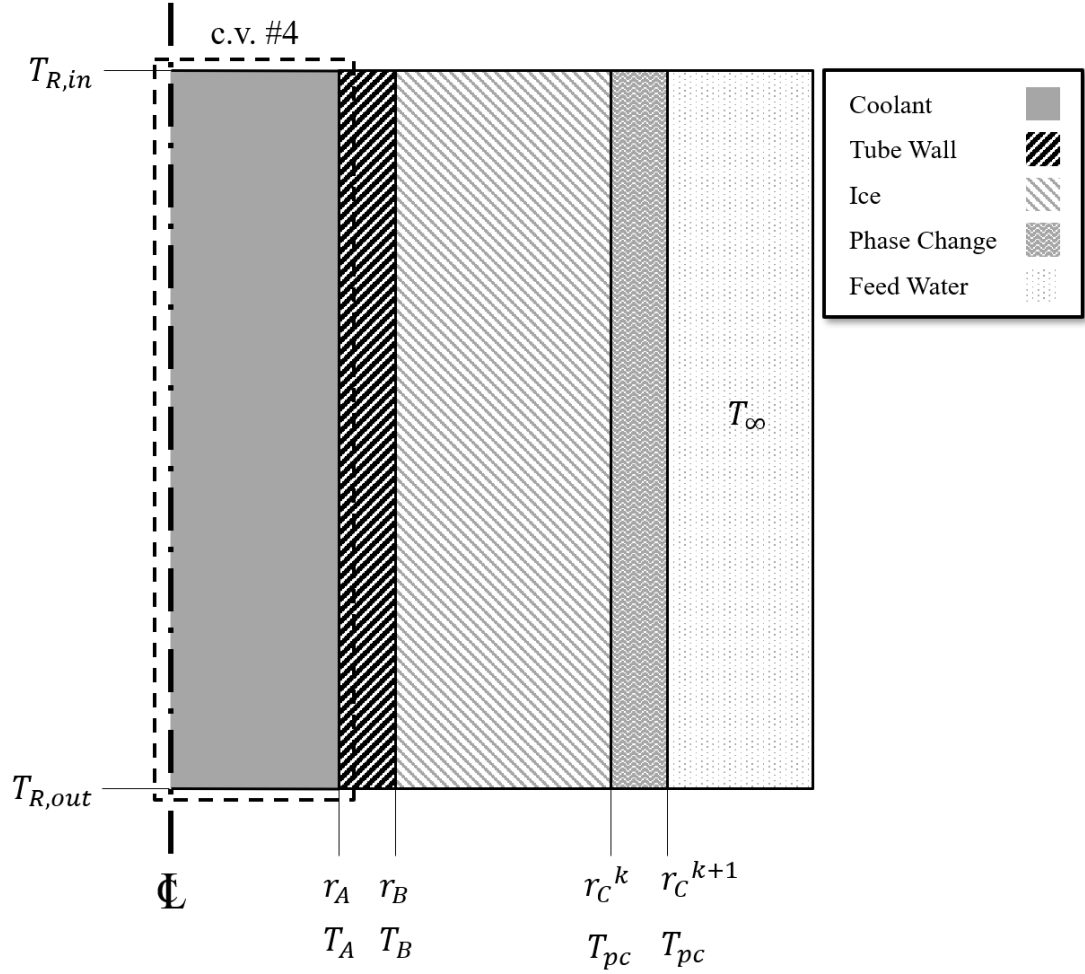


Figure 6: Control volume 4, around the coolant in the tube.

$$\frac{U_R^{k+1} - U_R^k}{\Delta t} = \dot{Q}_{conv,R} + \dot{m}_{RCR}(T_{R,in} - T_{R,out}) \quad (15)$$

where

$$\frac{U_R^{k+1} - U_R^k}{\Delta t} = \frac{\dot{m}_{RCR}}{\Delta t} \Delta T_{R,Avg} = \frac{\rho_R \pi r_A^2 L C_R}{\Delta t} (T_{R,Avg}^{k+1} - T_{R,Avg}^k) \quad (16)$$

and the superscripts k and $k + 1$ represent the property (U or T) at the previous and current time step, respectively. The energy balance can be rewritten as:

$$\frac{\rho_R \pi r_A^2 L c_R}{\Delta t} (T_{R,Avg}^{k+1} - T_{R,Avg}^k) = 2\pi r_A L h_R (T_A - T_{R,Avg}) + \dot{m}_{RCR} (T_{R,in} - T_{R,out}) \quad (17)$$

After assigning ΔV to the current time index, and temperature values to either current or previous time indices, the system of equations 7, 10, 13, 14, and 17 is the basis of the transient global analysis, from which $T_A, T_B, \Delta V, T_{R,Avg}$, and $T_{R,out}$ can be assessed at the $k + 1$ time step. From here, the constant terms in the equations can be collected in order to improve readability and make coding the system more simple. The resulting equations are:

$$\alpha(\Delta V_{ice}^{k+1}) = \beta(T_{pc} - T_B^{k+1}) \quad (18)$$

$$\beta(T_{pc} - T_B^{k+1}) = \delta(T_B^{k+1} - T_A^{k+1}) \quad (19)$$

$$\delta(T_B^{k+1} - T_A^{k+1}) = \epsilon(T_A^{k+1} - T_{R,Avg}^{k+1}) \quad (20)$$

$$T_{R,Avg}^{k+1} = \frac{T_{R,in}^{k+1} + T_{R,out}^{k+1}}{2} \quad (21)$$

$$\theta(T_{R,in}^{k+1} - T_{R,out}^{k+1}) = \epsilon(T_A^{k+1} - T_{R,Avg}^{k+1}) + \phi(T_{R,Avg}^{k+1} - T_{R,Avg}^k) \quad (22)$$

where the collected constants are,

$$\alpha = \frac{\rho_{ice}\lambda_{sf}}{\Delta t} \quad (23)$$

$$\beta = \frac{2\pi k_{ice}L}{\ln\left(\frac{r_C^k}{r_B}\right)} \quad (24)$$

$$\delta = \frac{2\pi k_w L}{\ln\left(\frac{r_B}{r_A}\right)} \quad (25)$$

$$\epsilon = 2\pi r_A L h_R \quad (26)$$

$$\phi = \frac{\rho_R \pi r_A^2 L c_R}{\Delta t} \quad (27)$$

$$\theta = \dot{m}_R c_R \quad (28)$$

Equations 18 through 22, with constants as defined in equations 23 through 28, can be written in matrix form, which represents the system of equations used

to analyze the transient global system. A list of all constant values can be found in Appendix E.

$$\begin{bmatrix} 0 & \beta & \alpha & 0 & 0 \\ \delta & -\beta + \delta & 0 & 0 & 0 \\ -\delta - \epsilon & \delta & 0 & \epsilon & 0 \\ -\epsilon & 0 & 0 & \phi + \epsilon & \theta \\ 0 & 0 & 0 & 2 & -1 \end{bmatrix} \begin{bmatrix} T_A^{k+1} \\ T_B^{k+1} \\ \Delta V_{ice}^{k+1} \\ T_{R,Avg}^{k+1} \\ T_{R,out}^{k+1} \end{bmatrix} = \begin{bmatrix} \beta T_{pc} \\ \beta T_{pc} \\ 0 \\ \phi T_{R,Avg}^k + \theta T_{R,in}^{k+1} \\ T_{R,in}^{k+1} \end{bmatrix}$$

Note that for the transient global analysis, $T_{R,in}^{k+1}$ is a constant. The justification for having a temperature at the $k+1$ timestep is discussed in section 3.3.

3.3 Spacial-Temporal Analysis

In the final analysis, a space discretization is added along the length of the tube. Thankfully, this analysis is the same as the transient global analysis and the same equations can be used to calculate ice growth over each length segment in the tube. In order to discretize in length, a differential length δL will be substituted for any appearance of L in the equations and all non-constant terms will be given a j subscript in order to index length segments. One important clarification with the spacial-temporal system is that while all the calculated values for T_A , T_B , r_C , and $T_{R,Avg}$ are still stored in the current length step (i.e. j), $T_{R,in}^{k+1}$ becomes $T_{R,j}^{k+1}$ and

$T_{R,out}^{k+1}$ becomes $T_{R,j+1}^{k+1}$. In this way, the coolant outlet temperature of one length segment becomes the inlet of the next length segment at the same time step, as would be expected. Thus, the system of equations can be written in matrix form as follows:

$$\begin{bmatrix} 0 & \beta & \alpha & 0 & 0 \\ \delta & -\beta + \delta & 0 & 0 & 0 \\ -\delta - \epsilon & \delta & 0 & \epsilon & 0 \\ -\epsilon & 0 & 0 & \phi + \epsilon & \theta \\ 0 & 0 & 0 & 2 & -1 \end{bmatrix} \begin{bmatrix} T_{A,j}^{k+1} \\ T_{B,j}^{k+1} \\ \Delta V_{ice,j}^{k+1} \\ T_{R,Avg,j}^{k+1} \\ T_{R,j+1}^{k+1} \end{bmatrix} = \begin{bmatrix} \beta T_{pc} \\ \beta T_{pc} \\ 0 \\ \phi T_{R,Avg,j}^k + \theta T_{R,j}^{k+1} \\ T_{R,j}^{k+1} \end{bmatrix}$$

Using the steady-state analysis, the transient system of equations, and the spacial-temporal system of equations, data can be generated for the different analyses at varying operating conditions. A Matlab code was developed that allows for all variables to be changed in order to analyze their effect on the system. In the next chapter, generated data will be presented. Reference Appendix A for the full Matlab code, using the above system of equations, for a spacial-temporal analysis.

4 RESULTS & DISCUSSION

Recall that the values for the base case were generated by a genetic learning algorithm used to optimize the system containing a chiller with cooling capacity of $4.1kW$ (restricted to 80% to account for losses) and maximum mass flow rate of $0.363\frac{kg}{s}$. Since the analyses are conducted on a single tube, cooling capacity and mass flow rate are divided over the total number of tubes in the freeze chamber. The calculated base case values are as follows:

Table 2: Base case (B.C.) values.

$Cycle\ Time(s)$	$L(m)$	$r_A(mm)$	$r_B(mm)$	$\dot{m}_{R,tube}\left(\frac{g}{s}\right)$	N_{tubes}
1,500	0.67	3.85	4.95	5.58	65

What is referred to in the table above as “Cycle Time” is the optimal length of the freezing process in seconds. Before data were generated, a convergence analysis was conducted for the space and time increments used to ensure low spacial and temporal error in the model. To assess convergence, the amount of total ice produced was the measure. The analysis was first run for the base case cycle time and tube length of 1,500s and 0.5m, respectively, a time increment of 100s, and a length increment of 100mm. The length increment was halved until relative error in ice volume fell below 0.1%, then the same was done with the time increment. This process was repeated until halving neither time nor length increments produced a relative error above the threshold. The final increments

for convergence were $\delta L = 0.00156m$ and $\delta t = 0.39s$. Results of the convergence analysis are shown in figure 7 and figure 8. Figure 7 shows the route taken by changing spacial and temporal step sizes to reach convergence, and figure 8 shows the total volume as a function of time for several $\delta L, \delta t$ combinations from figure 7.

Using the step size conditions that give a converged solution, the results for all three analyses are provided in figure 9. The figure displays the trend of ice growth on a single tube with respect to time for all three analyses conducted. The steady-state global analysis produces the most ice, as expected. Because the transient and spacial-temporal analyses produce such similar results, it may be difficult to distinguish the two in the figure. The most interesting part of this plot, perhaps, is how similar the transient global and spacial-temporal results are. The transient global analysis produces a constant thickness ice layer along the length of the tube, while the spacial-temporal analysis allows this thickness to change along the tube length. However, because the ice profile generated in the latter analysis is linear (see figure 10), the average ice thickness of this ice profile is almost exactly the same as the uniform thickness calculated in the transient global analysis. At $10,000s$, where the relative error between the two analyses is greatest, the average ice radius in the spacial-temporal analysis only differs from the transient uniform radius by $3.61 \times 10^{-5}m$ or 0.16%.

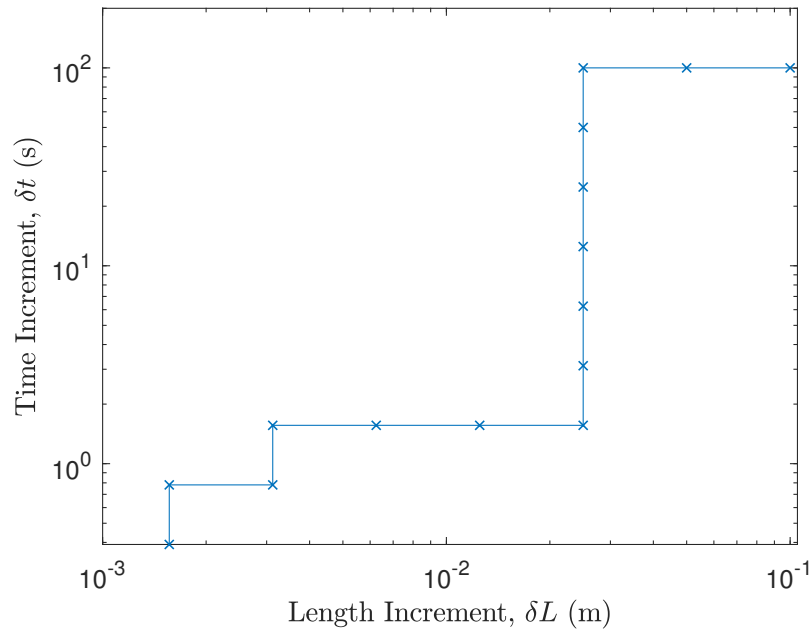


Figure 7: Tested conditions for δL and δt convergence.

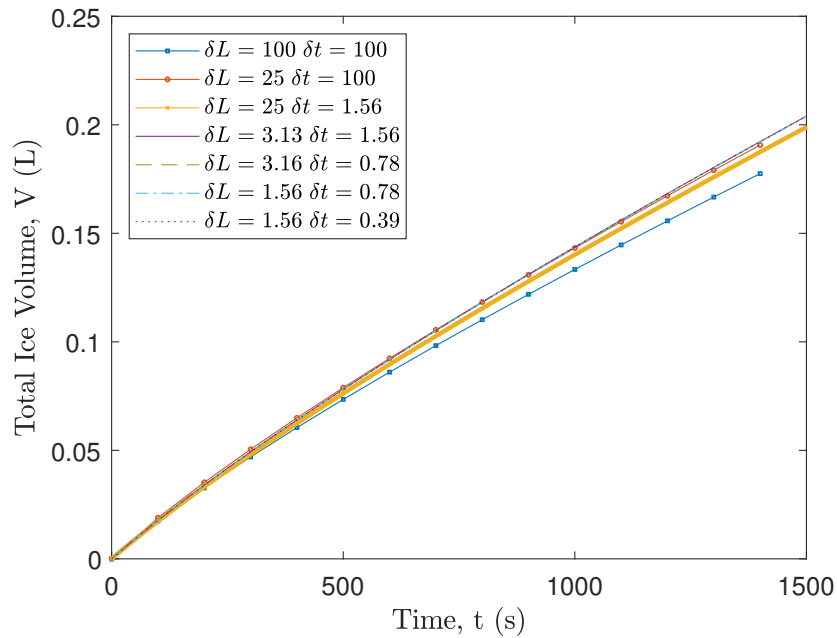


Figure 8: Volume of ice produced as a function of time at vertices of figure 7. Note that the code iterates in time between 0 and $(1500 - \delta t)$ seconds. This is not an issue at small time steps, but at larger time steps, the cycle time is cut short.

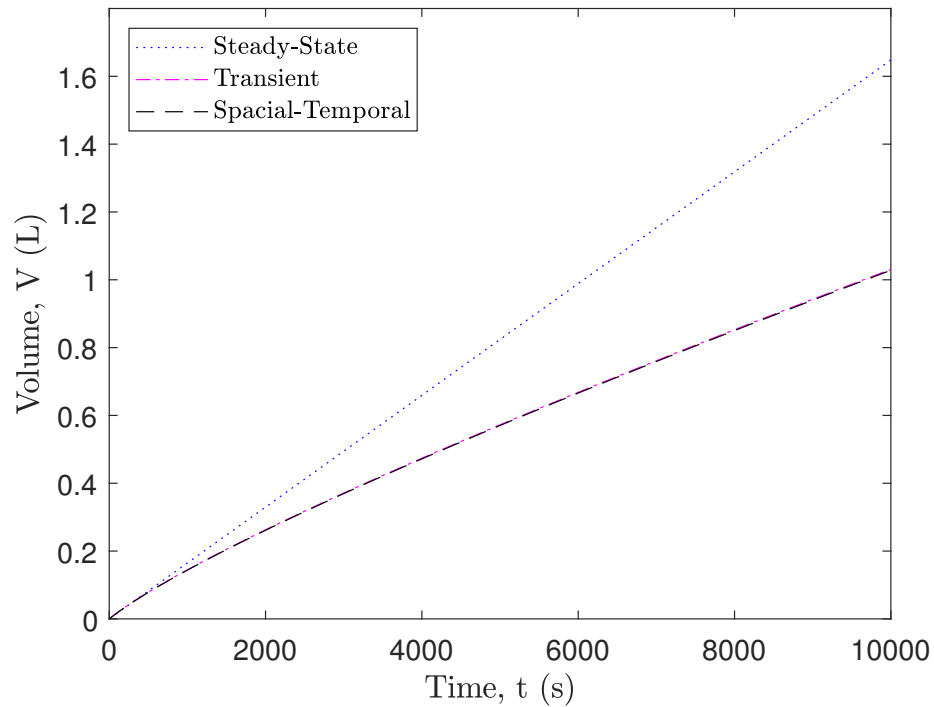


Figure 9: Ice production as a function of time for all three analyses.

It would be expected in an experimental setup for the ice growth rate to taper off dramatically with time. However, figure 9, which shows the volume of ice as a function of time does not reflect this. The taper is gradual, not dramatic, and a function of increasing thermal resistance through the ice layer; the thickness of which grows with time. This may be due, in part, to the lack of a convective term coming from the feed saltwater. While this term can be neglected over short time periods where the outer surface area of the ice is relatively small, as cycle time increases, this assumption may also affect the accuracy of the system. However, because it is known that in a realistic scenario ice production rate should decrease at longer cycle times due to the increasing thermal resistance of the ice layer, there

is no need to further investigate these cycle times that are significantly impacted by the zero convection assumption. Further results will only be presented at cycle times of 1,500s (B.C.) or less, where the system is most accurate.

With a converged solution, spacial-temporal results can be presented, starting with the base case conditions shown in figures 10, 11, and 12. Figure 10 shows how the ice profile along the length of the tube changes with time (note that the coolant inlet is at $z = 0.67m$ and the coolant outlet is at $z = 0m$). Because the coolant outlet temperature is warmer than the inlet, less ice is formed at the outlet than the inlet which produces the non-uniform ice profile shown. Figure 11 shows how the conductive resistance of the ice changes with time. As more ice is formed, the conductive resistance increases. Because of the decreasing ice thickness over the length of the tube, the thermal resistance also decreases closer to the outlet. Figure 12 shows how the rate of heat removal from the system by the coolant changes as a function of time. At $t = 0$ the thermal resistance is at a minimum because no ice has been formed yet. As the ice layer grows and thermal resistance increases, less heat is removed from the system by the coolant. At the base case conditions, $0.204L$ of ice is produced on a single tube, and a maximum of $3.68kW$ is rejected to the coolant by the phase change, as noted in figure 12 near the beginning of the cycle.

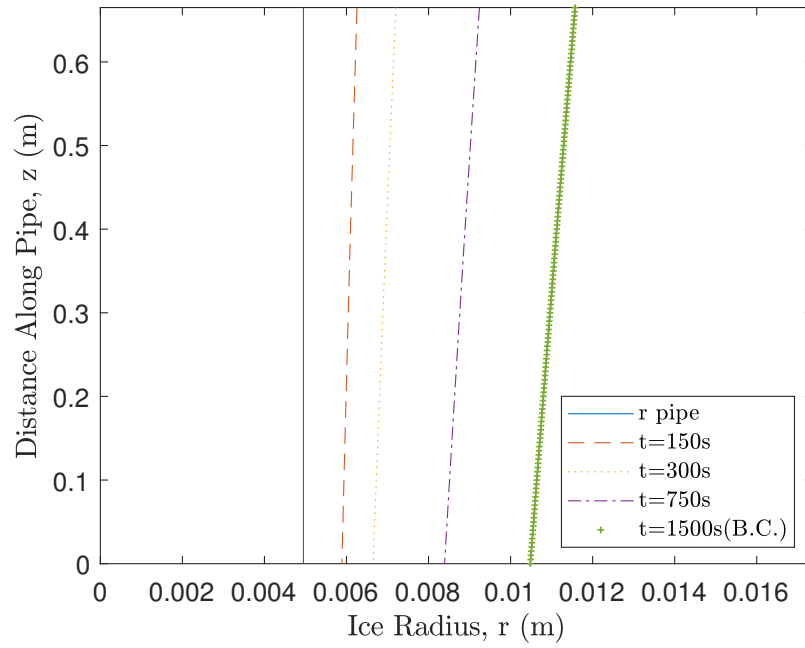


Figure 10: Ice growth profile along the tube length as a function of time.

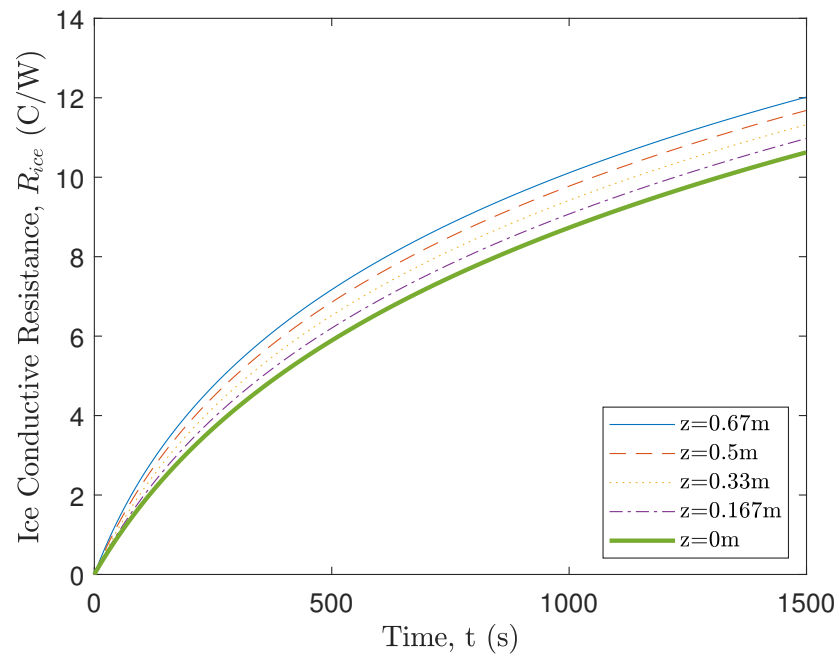


Figure 11: Conductive resistance of ice layer as a function of time at different points along the tube length.

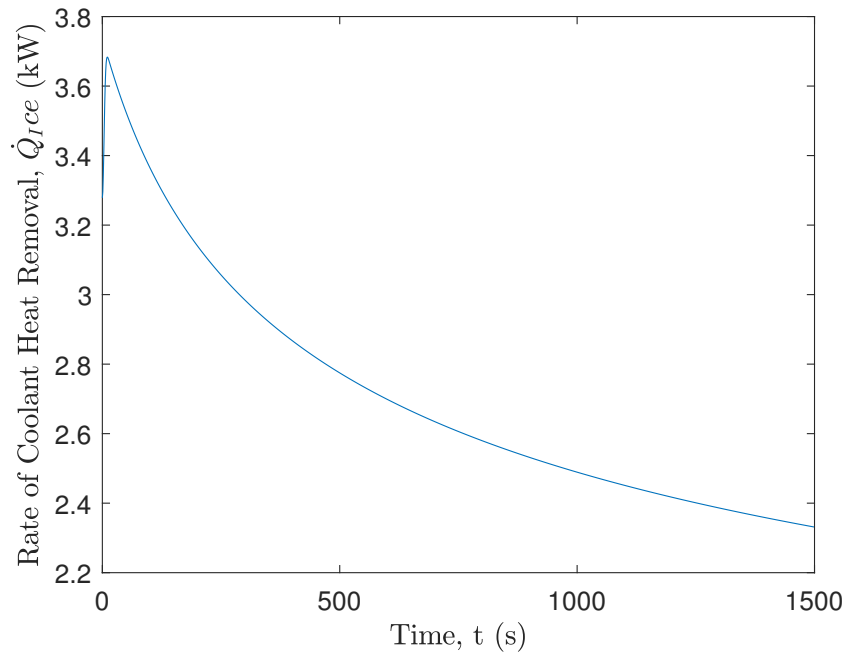


Figure 12: Coolant heat removal rate with respect to time at base case.

Figures 11 and 12 are somewhat linked in the fact that as the conductive resistance of the ice layer increases, less energy is being removed from the feed water. While the data suggests that shorter cycle times will have higher ice production rates, there are several reasons why extremely short cycle times are not practical. A certain “system changeover time” needs to be accounted for in order to understand why this is not the case. System changeover time refers to any time occupied between cycles by system stages. The stages may include, but are not limited to freeze chamber draining and freeze chamber refilling. Because of this, increasing the number of cycles also increases the total amount of system changeover in a given period of time. While the exact length of this changeover time cannot be determined without experimental testing, it is apparent that the longer the system changeover takes, the longer the cycle time needs to be in order to maximize daily

ice production. The system changeover time is not greatly concerning in regard to this research because it does not directly affect the results of the freeze analysis. However, the genetic learning algorithm optimized the system to maximize ice produced per day, which necessitates the use of some changeover time to keep the algorithm from favoring extremely low cycle times. For the purposes of optimizing the system, each time the freezing process was run, a subsequent melting process of the same cycle time was run, followed by a 10 minute changeover time. This is the reason for a base case cycle time of 1,500 seconds. In this way, the changeover time—which is hard to determine before experimental testing—will affect the performance of the system, but it is expected to be on a similar magnitude to the assumed value and is easy to account for once experimental data is obtained.

Figure 13 shows how the ice profile is changed as the coolant mass flow rate is changed. At higher mass flow rates, the temperature drop over the length of the tube is reduced and a more uniform thickness ice profile is developed. A more uniform ice profile increases ice production; however, the relationship between coolant mass flow rate and ice volume is not linear (reference figure 14). While more ice can be produced on a single tube by increasing the coolant mass flow rate, there are only two ways to increase coolant mass flow rate through individual tubes in this system: reduce the number of tubes in the freeze chamber or increase the chiller maximum mass flow rate by specifying a larger chiller unit. Because of the non-linear increase in ice production with increasing coolant mass flow rate, it is clear that reducing the number of tubes in order to increase mass flow rate will

result in a lower total ice production. Increasing chiller size comes at the cost of more total energy consumption and a larger impact on the space restraints of the overall design.

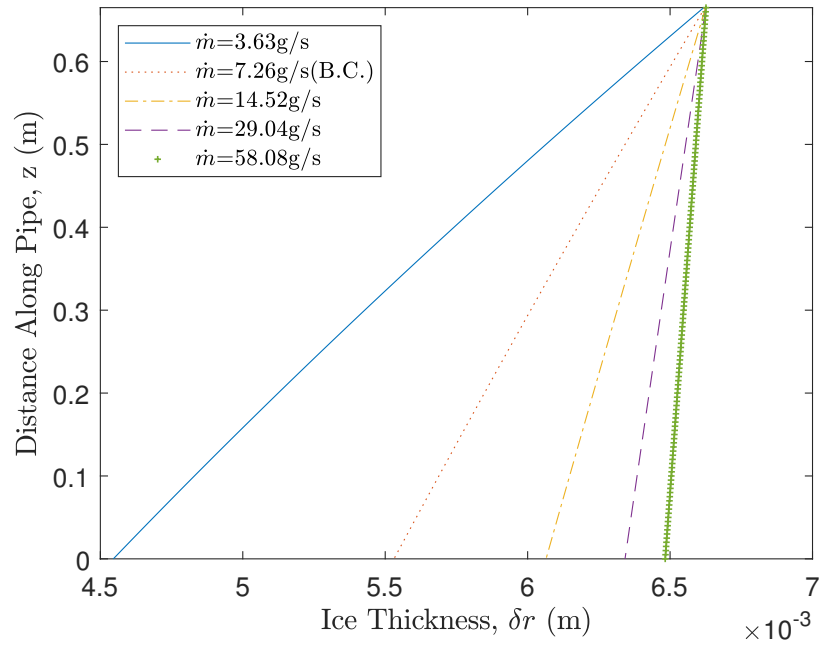


Figure 13: Ice profile along the length of the tube with varying coolant mass flow rate. Note that because the x-axis does not begin at zero, the shape of the ice profile is exaggerated.

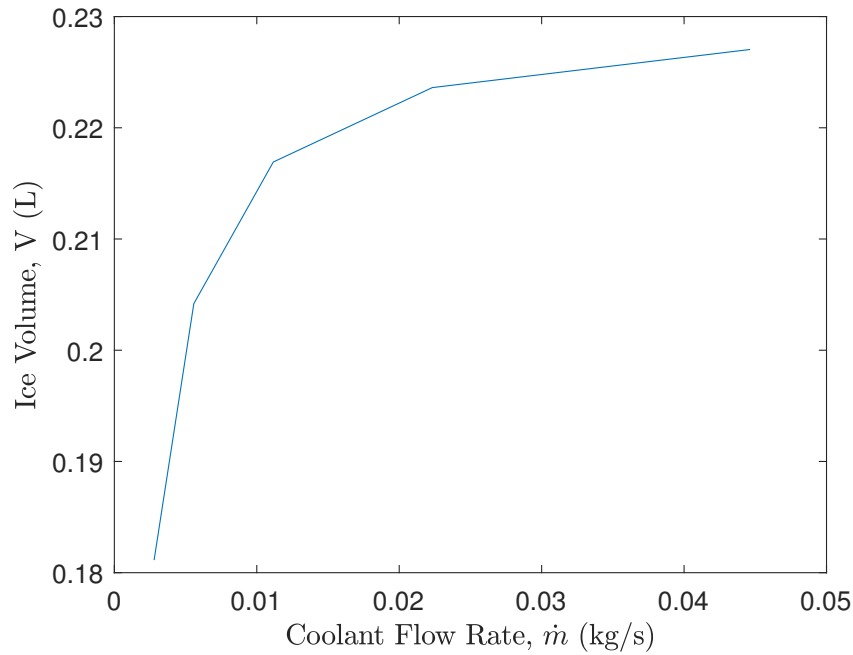


Figure 14: Volume of ice produced as a function of coolant mass flow rate.

Overall tube length is another variable that has a large effect of system performance. Figure 15 shows this effect while coolant mass flow rate is held constant at the inlet coolant temperature remains fixed at -10°C , allowing the required heat removal rate and exiting coolant temperature to fluctuate. While increasing tube length increases the amount of ice produced, figure 16 reveals that the power requirement from the chiller unit dramatically increases as tube length increases. Similar to the parametrization of the other system variables in this chapter, the trade-off between energy consumption and ice production doesn't allow for maximization or minimization of tube length—the optimal condition is an intermediate value ($0.67m$).

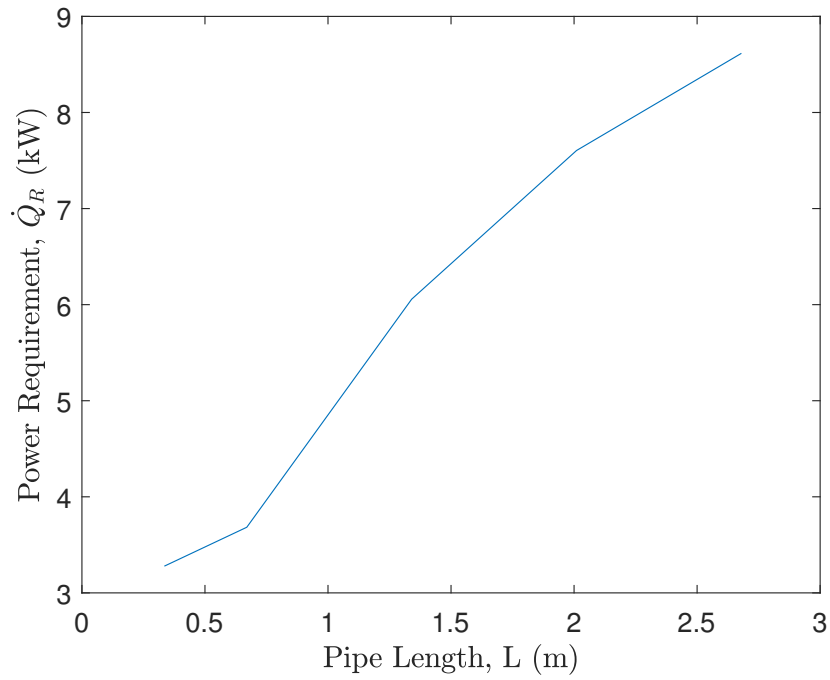


Figure 16: Chiller power requirement as a function of tube length.

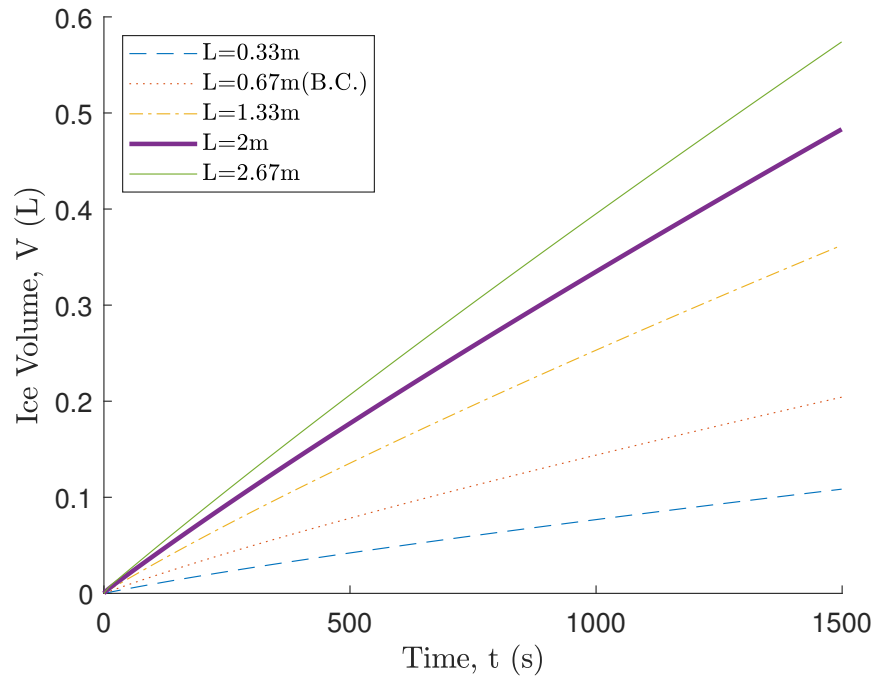


Figure 15: Volume of ice produced as a function of time with varying tube length.

The final variable parametrized in order to observe its effect on the system is outer tube radius, r_B . Figure 17 displays how the total amount of ice produced increases with tube radius for a fixed tube thickness. The trend shown in the plot can be explained by the fact that volume of ice produced is essentially a function of the total resistance between the coolant and the phase change region. Increasing the tube radius while holding tube thickness constant reduces the conductive resistance logarithmically ($R_{ice} = f \left[\ln \left(\frac{r_B}{r_A} \right) \right]$). Because the conductive resistance decreases logarithmically with increasing radius, larger tube sizes increase the total ice production at a decreasing rate, as is reflected in figure 17.

In order to understand why the genetic learning algorithm favored the base case radius over something larger, it is important to note that when parametrizing the outer radius of the tube to produce the data presented in figure 17, wall thickness was held constant while the tube radius varied freely. However, the genetic learning algorithm was forced to select options from a lookup table of commercially available tube sizes where wall thickness generally increases with diameter. The increased thermal resistance through the tube wall negatively impacts ice production rate. Because of the different constraints put on the numerical model parametrization and the genetic learning optimization, optimal conditions vary slightly. Also relevant to the overall system is the fact that when tube radius increases, the overall dimensions of the freeze chamber grow as well.

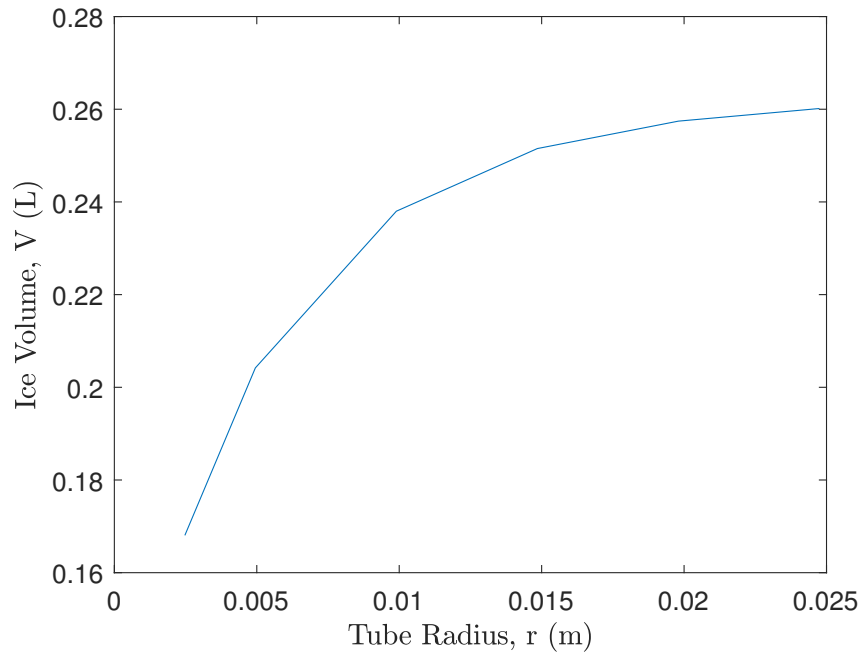


Figure 17: Volume of ice produced as a function of tube radius with tube thickness held constant.

As for the overall production capacity of the freezing process analyzed in this manuscript, a rough calculation can be completed to estimate the magnitude of its energy consumption and ice production capacity on a daily basis. This will allow for comparison to other methods and give the ability to give a preliminary determination of reliability, which is the ultimate goal of the research. Using the assumptions of a 10 minute system changeover time and equal cycle time/energy requirements for the melting cycle, daily ice production capacity is computed as follows:

$$\text{Daily Ice} \left(\frac{L}{\text{Day}} \right) = \frac{V_{Ice,tube} \times N_{tubes} \times \frac{\text{seconds}}{\text{day}}}{(2 \times \text{Cycle time}) + \text{Changeover time}} = \frac{0.204 \times 65 \times 86400}{(2 \times 1500) + 600}$$

This gives a total daily ice production of $318.2L \approx 0.32m^3$. The chiller specified in the overall system design that was used for the base case conditions has a power consumption of $6kW$. In order to make a more conservative estimate with regards to power consumed by the system, it will be assumed that $6kW$ is consumed by the system at every stage of the operation (freezing, melting, and changeover). This assumption is made to account for any energy consumed during the changeover process and gives a total daily energy consumption of $144kWh$. Thus, the energy requirement for the system is expected to be $0.453 \frac{kWh}{L} \approx 453 \frac{kWh}{m^3}$.

While comparing the energy requirements of this system to those of other methods presented in chapter 2.1 appears to discount the overall viability, the difference in efficiency between desalination plants that produce several million gallons per day and the one analyzed in this research is significant. It is more useful to compare systems of similar scale to determine viability. An example of a more comparable commercially available system is the Durastill 4280; a distiller that has a production rate of 42 gallons per day ($159L$) and a daily power consumption of $115.2kWh$ [16]. The resulting energy requirement per unit volume of fresh water produced is $725 \frac{kWh}{m^3}$. This is a much more reasonable comparison based on scale and shows that the indirect freezing system analyzed in this research is expected to perform significantly better than a distillation unit of the same scale.

5 CONCLUSIONS & RECOMMENDATIONS

The numerical model developed for this research provides a simple method for analyzing the freezing process of the proposed system. While improvements can certainly be made to increase accuracy, the model shows clearly how the system will react if certain conditions are perturbed. The parametrization of conditions like coolant mass flow rate, tube length, tube radius, and cycle length show trends in the system that are similar to what would be expected for an experimental model. This will allow for better design of an experimental model in the future, and save time and money related to design iterations. The tube in tank freeze desalination system proposed definitely indicates promise for the application and scale. Based on the analysis presented in this manuscript, further investigation into a small scale, portable, indirect freeze desalination unit is warranted.

From the numerical model parametrizations presented in this manuscript, several trends are expected from an experimental indirect tube-in-tank system. These trend expectations are summarized below:

- The rate of ice production with respect to time is not linear due to the increasing conductive resistance of the growing ice layer. The ice production rate slows with time and thus short cycle times are most efficient for the freezing process. However, recall that in the overall system, changeover time disallows minimization of cycle time.

- A more spacially uniform ice profile along the length of the tube can be achieved by increasing coolant mass flow rate. Because chiller energy requirements increase proportionally with coolant mass flow rate while total ice production increases with diminishing returns, coolant mass flow rate can be neither maximized nor minimized in the proposed system.
- Increased tube length will generally yield a larger volume of ice in a given time, at the cost of chiller energy consumption.
- Ice production increases logarithmically with tube radius so long as tube wall thickness remains constant. Increasing tube radius will also increase the overall size of the freeze chamber.

Each item above has its own consequence on the performance or design of the freezing process that prevents maximizing or minimizing any of the conditions. It is worth noting, however, that the model was optimized for maximum ice production per unit energy. It is possible to increase the overall production of the system by either increasing mass flow rate or tube length if ice production is valued over energy efficiency.

The numerical model developed as a part of this research could be made more robust in the future with several additions. A more realistic model would include considerations for the use of salt water as opposed to pure water in addition to including the convection between the ice and salt water in the tank. As ice is formed and the its salt content is rejected to the liquid water in the tank, not

only is the salinity of the liquid water increased, but—without some agitation—a concentration gradient is formed with maximum salinity closest to the ice. The paper written by Fujioka et al. [7] indicates a reduction in product water salinity as stirring velocity of the feed water in the tank increases. Adding a stirring component to the freeze chamber was not considered in the current research but should be included in any work moving forward, as the effect on product water salinity is notable. Of course, a stirring component will add to the energy consumption of the system, but it will perform much better with it because the number of necessary stages decreases as the reduction of product water salinity in each stage increases.

There are additional external factors not accounted for in the numerical analysis that will negatively impact the efficiency of an experimental model, but there are also several ways to improve the currently proposed system in future work. Perhaps the most significant energy saving improvement would be a reduction in the melting process. Since melting is only required to remove the ice from the tubes, the system could be designed in such a way as to let the ice slide off the tubes after the initial contact layer is melted. Once the ice is removed from the freeze chamber, ambient temperature could be used to fully melt the ice while another freezing cycle is started. Not only does this improvement save on the amount of energy consumed during the melting process, but also allows for more freezing cycles to be completed in a day.

Aside from improving the accuracy of the numerical model, the next step in proving system viability and verifying the analysis herein is an experimental test.

The small scale and simple design make the system extremely low cost and easy to replicate if chilling and heating units are available. Fully prototyping a mobile system, however, will require a significantly larger capital investment.

Finally, it is also worth mentioning the possibility of using a FM process as a pretreatment method for RO, because RO processes require pretreatment and do not perform well at high feed water salinity. It is possible that the use of a single FM cycle prior to the RO process could eliminate the need for additional pretreatment or posttreatment so long as the energy requirement of the FM process does not exceed that of the current methods used in RO.

REFERENCES

- [1] H. Perlman. The world's water. 2016. URL: <http://water.usgs.gov> (visited on 10/24/2017).
- [2] H. Perlman. Groundwater depletion. 2016. URL: <http://water.usgs.gov> (visited on 10/24/2017).
- [3] R. Prince. Water salinity and plant irrigation. 2016. URL: <http://www.agric.wa.gov.au> (visited on 01/25/2019).
- [4] H. Perlman. Saline water. 2016. URL: <http://water.usgs.gov> (visited on 01/25/2019).
- [5] EngineeringToolBox. Salinity of water. 2008. URL: https://www.engineeringtoolbox.com/water-salinity-d_1251.html (visited on 01/25/2019).
- [6] H. Curran. Water desalination by indirect freezing. *Desalination*, 7:273–284, 1969.
- [7] R. Fujioka, L. Wang, G. Dodbiba, and T. Fujita. Application of progressive freeze-concentration for desalination. *Desalination*, 319:33–37, 2013.
- [8] M. Pratt. Indirect freeze desalination melting analysis. *UHC Thesis, Oregon State University*, 2019.
- [9] A. K. Zander, M. Elimelech, D. H. Furukawa, P. Gleick, and K. R. Herd. *Desalination a national perspective*. National Academic Press, 2008. Washington, DC.
- [10] P. M. Williams, M. Ahmad, B. S. Connolly, and D. L. Oatley-Radcliffe. Technology for freeze concentration in the desalination industry. *Desalination*, 356:314–327, 2015.
- [11] P. M. Williams, M. Ahmad, and B. S. Connolly. Freeze desalination: an assessment of an ice maker machine for desalting brines. *Desalination*, 308:219–224, 2013.
- [12] W. E. Johnson. State-of-the-art of freezing processes, their potential and future. *Desalination*, 19:349–358, 1976.
- [13] H. Wiegandt and R. VonBerg. Myths about freeze desalination. *Desalination*, 33:287–297, 1980.
- [14] P. Schroeder, A. Chan, A. Khan, and A. Lloyd. Freezing processes-the standard of the future. *Desalination*, 21:125–136, 1977.
- [15] M. Rahman, M. Ahmed, and X. Chen. Freeze-melting process and desalination: review of the state-of-the-art. *Sep. Purif. Rev.*, 35:59–96, 2006.
- [16] Durastill 42 gpd automatic water distiller with 80 gallon reserve tank model 4280. 2019. URL: <http://www.h2olabs.com/p-259-42-gallon-per-day-automatic-with-80-gallon-reserve.aspx> (visited on 02/24/2019).

APPENDICES

Appendix A - Spacial-Temporal Analysis Code

```

%%~~~~~
%System Constants
%~~~~~

clear

fileID = fopen('SETUP.txt');
SETUP = fscanf(fileID, '%*s %*s %*s %*s %*s %*s %*s %*s
    %*s %f %*s
    %f %*s %f %*s %f %*s %f %*s %f %*s %f %*s %f %*s %f %*s %f
    %*s %f %*s %f %*s %f %*s %f %*s %f %*s %f %*s %f %*s %f');

%Variable Setup
Cycles = SETUP(14:end);           %[s] Cycle
    times to be tested.
Length = SETUP(6);                %[m]
    Total pipe length
L = SETUP(7);                     %[m] Length
    increment
L_vector = 0:L:Length;            %[m] Vector of
    discretized lengths
DELTAT = SETUP(1);                %[s]
    System timestep

Daily_Cycles = zeros(1,length(Cycles));
Daily_Ice = zeros(1,length(Cycles));
V_total = zeros(Cycles(end)/DELTAT,length(Cycles));

```

```

T_A = zeros((length(L_vector)-1),Cycles(end)/DELTAT ,
            length(Cycles));
T_B = zeros((length(L_vector)-1),Cycles(end)/DELTAT ,
            length(Cycles));
r_C = zeros((length(L_vector)-1),Cycles(end)/DELTAT ,
            length(Cycles));
T_R_avg = zeros((length(L_vector)-1),Cycles(end)/DELTAT ,
                length(Cycles));
Delta_V = zeros((length(L_vector)-1),Cycles(end)/DELTAT ,
                length(Cycles));
V_ice = zeros((length(L_vector)-1),Cycles(end)/DELTAT ,
                length(Cycles));
T_R = zeros(length(L_vector),Cycles(end)/DELTAT ,length(
            Cycles));

for k=1:length(Cycles)
    %%~~~~~
    %%Cycle Time Iteration
    %%~~~~~
    Cycle_Length = Cycles(k);                %[s] Length
        of freezing cycle
    t_vector = 0:DELTAT:Cycle_Length;        %[s] System
        run time
    Recharge_Time = Cycle_Length + 600;      %[s] Time to
        recharge system in between cycles
    Daily_Cycles(k) = floor(24*60*60/(Cycle_Length +
        Recharge_Time));    % Number of cycles that can
        be completed in 1 day

    %Overall
    T_pc = SETUP(2);                        %[C]
        Temperature of phase change
    T_inf = SETUP(3);                       %[C]
        Saltwater inlet temperature. Keep close to T_pc
        for system simplicity
    T_R(1,:,k) = SETUP(4);                  %[C] Inlet temperature of
        refrigerant at L=0
    T_R(:,1,k) = linspace(SETUP(4),SETUP(4)+SETUP(5),
        length(L_vector));
    T_A(:,1,k) = T_inf;
    T_B(:,1,k) = T_inf;

    %Pipes

```

```

r_A = SETUP(8);           %[m] Tube inner radius
    First analysis used 3/4 Type M copper tube: D =
    0.020599 t = 0.001
r_B = SETUP(9);           %[m] Tube outer radius
r_C(:,1,k) = r_B + 0.000001;    %[m] Added 0.1mm
    because equation for thermal resistance of ice
    fails if no ice at start Ice initial radius

k_W = 61;                 %[W/m-C] Thermal
    conductivity of tube stainless steel 1%

%Fluids
%Refrigerant
rho_R = SETUP(10);        %[kg/m^3] Density of
    refrigerant
c_R = SETUP(11);          %[J/g-C] Specific heat
    of refrigerant
h_R = SETUP(12);          %[W/m^2-C] Convective
    HTC of refrigerant assuming closer to constant q
    '' than constant T
m_dot_R = SETUP(13);      %[kg/s] Mass flow rate
    of refrigerant First analysis used N = 100 pipes
    with total mass flow 12.57 kg/min

%Water/Ice
k_I = 2.25;                %[W/m-C] Conductive resistance
    of ice
h_sf = 333300;            %[J/kg] Enthalpy of fusion of
    salt water assuming hsf_water = hsf_saltwater
h_s = 0;                  %[W/m^2-C] Neglect convection
    from saltwater in tank
rho_I = 917.4;            %[kg/m^3] Density of ice

for j=1:(length(t_vector)-1)
    %%
    for i=1:(length(L_vector)-1)           %This
        for loop iterates the system of equations by
        the given time step
            %% ~~~~~
            %System of Equations/Time Iteration
            %~~~~~
            if j==1

```

```

        T_R_avg(i,j,k) = (T_R(i+1,j,k) + T_R(i,j
            ,k))/2;     %[C] Initial average
                       temperature
    else
    end

    alpha = -1 * rho_I * h_sf / DELTAT;
    beta = -2 * pi * k_I * L / (log(r_C(i,j,k) /
        r_B));
    delta = 2 * pi * k_W * L / (log(r_B / r_A));
    epsilon = 2 * pi * r_A * L * h_R;
    phi = (rho_R * pi * ((r_A)^2) * L * c_R /
        DELTAT) * 1000;
    theta = m_dot_R * c_R * 1000;

                                 %Not
    included in eqn derivations, added for
    neatness

    Equations = [0, beta, alpha, 0, 0; delta, -
        delta+beta, 0, 0, 0; -delta-epsilon,
        delta, 0, epsilon, 0; -epsilon, 0, 0, phi
        +epsilon, theta; 0, 0, 0, 2, -1];
    Knowns = [beta*T_pc; beta*T_pc; 0; phi*
        T_R_avg(i,j,k)+theta*T_R(i,j,k); T_R(i,j,
        k)];
    Solutions = Equations\Knowns;

    if j<=(length(t_vector)-2)     %This if
        statement puts the time variant S.O.E.
        outputs where they belong
        T_A(i,j+1,k) = Solutions(1);
        T_B(i,j+1,k) = Solutions(2);
        Delta_V(i,j+1,k) = Solutions(3) * 1000;
        T_R_avg(i,j+1,k) = Solutions(4);
        V_ice(i,j+1,k) = V_ice(i,j,k) + Delta_V(
            i,j+1,k);     %[L] Volume of
                       ice produced
        r_C(i,j+1,k) = sqrt((Delta_V(i,j+1,k)
            /(1000*pi*L)) + (r_C(i,j,k)^2));
    else
    end

```

```

        if i<=(length(L_vector)-1) && j>1    %This if
            statement does the same as above for
            length variant outputs
            T_R(i+1,j,k) = Solutions(5);
        else
        end

    end
    if j<(length(t_vector)-1)
        V_total(j+1,k) = sum(V_ice(:,j+1,k));
    else
    end
    Daily_Ice(k) = Daily_Cycles(k) * V_total(length(
        t_vector)-1,k);
end
end

figure(1)
plot(Cycles,Daily_Ice,'--k')

[value,index] = find(Daily_Ice==(max(Daily_Ice)));

print_str = strcat('Full analysis optimal cycle time:',
    num2str(Cycles(index)), ' s\nTotal ice production/day:
    ',num2str(max(Daily_Ice)), ' L\n');

fprintf(print_str)

hold on

figure(2)
plot(t_vector(2:end),V_total(1:end,end),'--k')

hold on

```



```

T_R_avg = zeros(1,(length(Run_Time)-1));
T_R_out = zeros(1,(length(Run_Time)-1));
T_R_in = zeros(1,(length(Run_Time)));

%Overall
T_pc = SETUP(2);           %[C]
    Temperature of phase change
T_inf = SETUP(3);         %[C]
    Saltwater inlet temperature. Keep close to T_pc
    for system simplicity
T_R_in(:) = SETUP(4);     %[C]
    Inlet temperature of refrigerant
T_R_out(:,1) = T_R_in(1) + SETUP(5);   %[C]
    Initial outlet temperature of refrigerant
T_A(1) = T_inf;           %[C] Inner pipe wall
    temperature
T_B(1) = T_A(1);         %[C] Outer pipe wall
    temperature
T_R_avg(1) = (T_R_out(1) + T_R_in(1))/2;   %[C]
    Initial average temperature

%Pipes
L = SETUP(6);             %[m] Tube length
r_A = SETUP(8);           %[m] Tube inner radius
    First analysis used 3/4 Type M copper tube: D =
    0.020599 t = 0.001
r_B = SETUP(9);           %[m] Tube outer radius
r_C(p,1) = r_B + 0.000001;   %[m] Added 1mm
    because ln equation for thermal resistance of ice
    fails if no ice at start Ice initial radius

k_W = 61;                 %[W/m-C] Thermal
    conductivity of tube stainless steel 1%

%Fluids
%Refrigerant
rho_R = SETUP(10);        %[kg/m^3] Density
    of refrigerant
c_R = SETUP(11);          %[j/g-C] Specific
    heat of refrigerant
h_R = SETUP(12);          %[W/m^2-C]
    Convective HTC of refrigerant assuming closer
    to constant q'' than constant T

```

```

m_dot_R = SETUP(13);           %[kg/s] Mass flow
                                rate of refrigerant First analysis used N =
                                100 pipes with total mass flow 12.57 kg/min

%Water/Ice
k_I = 2.25;                     %[W/m-C] Conductive
                                resistance of ice
h_sf = 333300;                 %[J/kg] Enthalpy of fusion
                                of salt water assuming hsf_water =
                                hsf_saltwater
h_s = 0;                       %[W/m^2-C] Neglect convection
                                from saltwater in tank
rho_I = 917.4;                 %[kg/m^3] Density of ice

%%~~~~~
%System of Equations
%~~~~~
for j=1:(length(Run_Time)-1)   %This For
                                loop iterates the system of equations by the
                                given time step

    alpha = -1 * rho_I * h_sf / DELTAT;
    beta = -2 * pi * k_I * L / (log(r_C(p,j) / r_B))
    ;
    delta = 2 * pi * k_W * L / (log(r_B / r_A));
    epsilon = 2 * pi * r_A * L * h_R;
    phi = (rho_R * pi * ((r_A)^2) * L * c_R / DELTAT
    ) * 1000;
    theta = m_dot_R * c_R * 1000;

                                %Not included
                                in eqn derivations, added for neatness

    Equations = [0, beta, alpha, 0, 0; delta, -delta
    +beta, 0, 0, 0; -delta-epsilon, delta, 0,
    epsilon, 0; -epsilon, 0, 0, phi+epsilon,
    theta; 0, 0, 0, 2, -1];
    Knowns = [beta*T_pc; beta*T_pc; 0; phi*T_R_avg(j)
    +theta*T_R_in(j); T_R_in(j)];
    Solutions = Equations\Knowns;

    T_A(j+1) = Solutions(1);
    T_B(j+1) = Solutions(2);
    T_R_avg(j+1) = Solutions(4);
    T_R_out(j+1) = Solutions(5);

```

```

        Delta_V(p,j+1) = Solutions(3) * 1000;

        V_ice(p,j+1) = V_ice(p,j) + Delta_V(p,j+1);
                    % [L] Volume of ice produced
        r_C(p,j+1) = sqrt((V_ice(p,j+1)/(1000*pi*L)) + (
                    r_B^2));
    end

    %% ~~~~~
    % Performance Calculations
    % ~~~~~

    N_cycles(p) = floor(24*60*60 / (Cycle_Length +
        Recharge_Time)); % Gives number of
        cycles that can be run in 1 day

    V_Ice_Day(p) = N_cycles(p) * V_ice(p,length(Run_Time
        ));

end

figure(1)
plot(Cycles,V_Ice_Day,'-m')

[value,index] = find(V_Ice_Day==(max(V_Ice_Day)));

print_str = strcat('Time variant analysis optimal cycle
    time:',num2str(Cycles(index)),' s\nTotal ice
    production/day:',num2str(max(V_Ice_Day)),' L\n');

fprintf(print_str)

hold on

figure(2)
plot(Run_Time,V_ice(p,:),'-m')

hold on

```

Appendix C - Steady-State Analysis Code

```

clear

fileID = fopen('SETUP.txt');
SETUP = fscanf(fileID, '%*s %*s %*s %*s %*s %*s %*s %*s
    %*s %f %*s
    %f %*s %f %*s %f %*s %f %*s %f %*s %f %*s %f %*s %f %*s %f
    %*s %f %*s %f %*s %f %*s %f %*s %f %*s %f %*s %f %*s %f');

cycles = SETUP(14:end); %[s]
    Cycle times to be tested

N_cycles = zeros(1, length(cycles));
V_Ice_Day = zeros(1, length(cycles));
V = zeros(1, length(cycles));

for p=1:length(cycles)

    V_ice(1) = 0;

    rho_I = 917.4; %[kg/m
        ^3] Density of ice
    h_sf = 333300; %[J/kg]
        Enthalpy of fusion of salt water assuming
        hsf_water = hsf_saltwater
    L = SETUP(6); %
        [m] Tube length
    r_B = SETUP(9); %[m] Tube outer radius
    r_C(1) = r_B; %[m]
        Starting ice radius (0)
    T_pc = SETUP(2); %[
        C] Temperature of phase change
    T_R_in = SETUP(4); %[C
        ] Inlet temperature of refrigerant
    T_R_out = T_R_in + SETUP(5); %[C]
        Initial outlet temperature of refrigerant
    m_dot_R = SETUP(13); %[kg/s] Mass flow rate
        of refrigerant First analysis used N = 100 pipes
        with total mass flow 12.57 kg/min
    c_R = SETUP(11) * 1000; %[J/kg-C]
        Specific heat of refrigerant

    alpha = rho_I * h_sf / cycles(p);

```

```
V_ice(2) = (m_dot_R * c_R / alpha) * (T_R_out -
          T_R_in) * 1000;

V(p) = V_ice(2);

N_cycles(p) = floor(24*60*60 / (2 * cycles(p) + 600)
);           %Gives number of cycles that can be
            run in 1 day

V_Ice_Day(p) = N_cycles(p) * V_ice(2);
end

figure(1)
plot(cycles,V_Ice_Day,':b')

[value,index] = find(V_Ice_Day==(max(V_Ice_Day)));

print_str = strcat('Global analysis optimal cycle time:'
, num2str(cycles(index)), ' s\nTotal ice production/day
:', num2str(max(V_Ice_Day)), ' L\n');

fprintf(print_str)

hold on

figure(2)

plot(cycles,V,':b')

hold on
```

Appendix D - Convergence Analysis Code

```

clc
clear
close all

%% Basic condition values

bc_time = 1500;    %[s] cycle time
bc_length_pipe = 0.67; %[m] pipe overall length
bc_lstep = 0.1;   %[m] length increment
bc_tstep = 100;   %[s] time increment
bc_t_infinity = -1.9;    %[C] saltwater tank temperature
bc_delta_temp = 2.49;   %[C] delta t provided by chiller
bc_inner_rad = 0.00385; %[m] inner pipe radius
bc_outer_rad = 0.00495; %[m] outer pipe radius
bc_mass_flow = 0.00558; %[kg/s] coolant mass flow rate

time = bc_time;    %[s] cycle time
length_pipe = bc_length_pipe; %[m] pipe overall length
lstep = bc_lstep;  %[m] length increment
tstep = bc_tstep;  %[s] time increment
t_infinity = bc_t_infinity;    %[C] saltwater tank
    temperature
delta_temp = bc_delta_temp;    %[C] delta t provided by
    chiller
inner_rad = bc_inner_rad;    %[m] inner pipe radius
outer_rad = bc_outer_rad;    %[m] outer pipe radius
mass_flow = bc_mass_flow;    %[kg/s] coolant mass flow
    rate

[~,~,V_func,t_func,~,~,~]=Full_Func_2(time,length_pipe,
    lstep,tstep,t_infinity,delta_temp,inner_rad,outer_rad
    ,mass_flow);

V(1,1:length(V_func)) = V_func;
t(1,:) = t_func(1:end-1);
relerr(1) = 100;
k=1;
loop = [100,100];
tstepplot(k) = tstep;
lstepplot(k) = lstep;

while loop(1)>1 || loop(2)>1

```

```
    errtemp = relerr(k);
    relerr(k) = 100;

    loop(1)=0;
    while relerr(k)>0.1

        relerr(k-loop(1)) = errtemp;

        lstep = lstep/2;

        [~,~,V_func,t_func,~,~,~]=Full_Func_2(time,
            length_pipe,lstep,tstep,t_infinity,delta_temp
            ,inner_rad,outer_rad,mass_flow);

        k = k+1;
        tstepplot(k) = tstep;
        lstepplot(k) = lstep;

        V(k,1:length(V_func)) = V_func;
        t(k,1:length(t_func(1:end-1))) = t_func(1:end-1)
            ;

        relerr(k) = abs((V(k,end)-max(V(k-1,:)))/(V(k,
            end))*100);

        loop(1)=loop(1)+1;
    end

    errtemp = relerr(k);
    relerr(k) = 100;

    loop(2)=0;
    while relerr(k)>0.1

        relerr(k-loop(2)) = errtemp;

        tstep = tstep/2;

        [~,~,V_func,t_func,~,~,~]=Full_Func_2(time,
            length_pipe,lstep,tstep,t_infinity,delta_temp
            ,inner_rad,outer_rad,mass_flow);

        k = k+1;
```

```

        tstepplot(k) = tstep;
        lstepplot(k) = lstep;

        V(k,1:length(V_func)) = V_func;
        t(k,1:length(t_func(1:end-1))) = t_func(1:end-1)
        ;

        relerr(k) = abs((V(k,end)-max(V(k-1,:)))/(V(k,
            end))*100);

        loop(2)=loop(2)+1;
    end
end
figure (1)
plot(lstepplot,tstepplot,'-x')
set(gca,'Yscale','log')
set(gca,'Xscale','log')
set(gca,'FontSize',12)
xlim([0.001 0.105])
ylim([0 200])
xlabel('Length Increment,  $\Delta L$  (m)','Interpreter','
    latex')
set(gca,'FontSize',12)
ylabel('Time Increment,  $\Delta t$  (s)','Interpreter','
    latex')
figure (2)
plot(t(1,1:15),V(1,1:15),'-s','markersize',2)
hold on
plot(t(3,1:15),V(3,1:15),'-o','markersize',2)
plot(t(9,1:960),V(9,1:960),'-x','markersize',2)
plot(t(12,1:960),V(12,1:960))
plot(t(13,1:1920),V(13,1:1920),'--')
plot(t(14,1:1920),V(14,1:1920),'-.'')
plot(t(15,1:3840),V(15,1:3840),':')
set(gca,'FontSize',12)
legend('$\Delta L=100 \backslash; \Delta t=100$', '$\Delta L=25 \backslash;
    \Delta t=100$', '$\Delta L=25 \backslash; \Delta t=1.56$', '$\Delta
    L=3.13 \backslash; \Delta t=1.56$', '$\Delta L=3.16 \backslash; \Delta
    t=0.78$', '$\Delta L=1.56 \backslash; \Delta t=0.78$', '$\Delta
    L=1.56 \backslash; \Delta t=0.39$', 'Location','northwest
    ','Interpreter','latex')
xlabel('Time, t (s)','Interpreter','latex')
ylabel('Total Ice Volume, V (L)','Interpreter','latex')

```

Appendix E - Base Case System Constants

Table 3: Base case (B.C.) constants.

Name	Value
T_{pc}	$0\text{ }^{\circ}\text{C}$
$T_{R,in}$	$-10\text{ }^{\circ}\text{C}$
r_A	$0.00385m$
r_B	$0.00495m$
ρ_R	$1047\frac{kg}{m^3}$
c_R	$3.627\frac{J}{kg-C}$
h_R	$550\frac{W}{m^2-K}$
$\dot{m}_{R,pipe}$	$0.00558\frac{kg}{s}$
k_W	$61\frac{W}{m-C}$
k_{ice}	$2.25\frac{W}{m-C}$
λ_{sf}	$333,000\frac{J}{kg}$
ρ_I	$916\frac{kg}{m^3}$

